

**MULTIMODE-MULTILEVEL BIDIRECTIONAL TARGETED BATTERY
VOLTAGE EQUALIZER FOR SERIES CONNECTED BATTERY UNITS**

DISSERTATION/THESIS

SUBMITTED IN PARTIAL FULFILLMENT OF THE REQUIREMENTS
FOR THE AWARD OF THE DEGREE
OF

MASTER OF TECHNOLOGY
IN
POWER ELECTRONICS & SYSTEMS

Submitted by:

SHREEPOOJA SINGH

2k20/PES/20

Under the supervision of

PROF. VISHAL VERMA
(Professor, EED, DTU)



DEPARTMENT OF ELECTRICAL ENGINEERING
DELHI TECHNOLOGICAL UNIVERSITY

(Formerly Delhi College of Engineering)
Bawana Road, Delhi-110042

MAY, 2022

DEPARTMENT OF ELECTRICAL ENGINEERING

DELHI TECHNOLOGICAL UNIVERSITY

(Formerly Delhi College of Engineering)

Bawana Road, Delhi-110042

CANDIDATE'S DECLARATION

I, **SHREEPOOJA SINGH**, Roll No. 2k20/PES/20 student of M.Tech (Power Electronics & System), hereby declare that the project Dissertation titled “**Multimode-Multilevel Bidirectional Targeted Battery Voltage Equalizer for Series Connected Battery Units**” which is submitted by me to the Department of Electrical Engineering Department, Delhi Technological University, Delhi in partial fulfillment of the requirement for the award of the degree of Master of Technology, is original and not copied from any source without proper citation. This work has not previously submitted for the award of any Degree, Diploma.

Place: Delhi

(Shreepooja Singh)

Date:

DEPARTMENT OF ELECTRICAL ENGINEERING

DELHI TECHNOLOGICAL UNIVERSITY

(Formerly Delhi College of Engineering)

Bawana Road, Delhi-110042

CERTIFICATE

I hereby certify that the Project Dissertation titled “**Multimode-Multilevel Bidirectional Targeted Battery Voltage Equalizer for Series Connected Battery Units**” which is submitted by **SHREEPOOJA SINGH**, Roll No. 2K20/PES/20, Department of Electrical Engineering, Delhi Technological University, Delhi in partial fulfillment of the requirement for the award of the degree of Master of Technology, is a record of the project work carried out by the student under my supervision. To the best of my knowledge this work has not been submitted in part or full for any Degree or Diploma to this University or elsewhere.

Place: Delhi

Date:

PROF. VISHAL VERMA

(SUPERVISOR)

ACKNOWLEDGEMENT

I would like to express my gratitude towards all the people who have contributed their precious time and effort to help me without whom it would not have been possible for me to understand and complete the project.

I would like to thank **Prof. Vishal Verma** (Professor, Department of Electrical Engineering, DTU, Delhi) my Project guide, for supporting, motivating and encouraging me throughout the period of this work was carried out. His readiness for consultation at all times, his educative comments, his concern and assistance even with practical things have been invaluable.

Besides my supervisor, I would like to thank all the PhD. scholars of **Simulation Lab**, for helping me wherever required and provided me continuous motivation during my research.

Finally, I must express my very profound gratitude to my parents, seniors and to my friends for providing me with unfailing support and continuous encouragement throughout the research work.

Date: 31/05/22

Shreepooja Singh
M.Tech (Power Electronics & System)
Roll No. 2K20/PES/20

ABSTRACT

With the government enacting several initiatives to reduce pollution and encourage green energy, the percentage of renewables in the nation's power capacity composition is certain to rise. However, numerous concerns and obstacles must be overcome before renewable energy can be seamlessly integrated into the Indian Power Grid. Energy storage is critical in such circumstances to balance the risks of renewables, enhancing overall system dependability and offering other ancillary services. To achieve voltage requirements, several lead acid battery cells are commonly linked in series. The voltages of all serially linked battery cells in a battery pack should be the same for optimum performance. However, such an outcome is unachievable in real life owing to inescapable factors. Unbalanced battery cell voltages can lower storage capacities and, in the worst-case scenario, produce explosions or fires, which is a severe impediment to safe and optimal battery operation. As a result, battery cell voltage equalizations have emerged as a critical study area. Battery equalizers improve battery life-cycle and safety.

This research study proposes Multimode-Multilevel Bidirectional Converter (MMBE) and Multi-looped Current-controlled Bidirectional Bridge converter (MCBB), two new active voltage equalizers that can operate multiple legs at a time along with its auxiliary circuits for achieving faster and targeted balancing. Switching algorithm of the converter is effectively controlled by setting the thresholds of voltage difference and enabling multiple current loops to target the energy flow towards the weakest cells with customized gradients. The proposed topology and control are implemented on the MATLAB platform, and the results confirm the effectiveness and quick dynamics of the proposed equalization system.

TABLE OF CONTENTS

CANDIDATE DECLARATION	II
CERTIFICATE	III
ACKNOWLEDGEMENT	IV
ABSTRACT	V
TABLE OF CONTENTS	VI
LIST OF FIGURES	IX
LIST OF TABLES	XI
LIST OF ABBREVIATIONS	XII
LIST OF SYMBOLS	XIII
CHAPTER-1: INTRODUCTION	1
1.1 Need for Renewable Power Systems	1
1.2 Importance of Battery Energy Storage Systems (ESS)	4
1.3 Requirement of Battery Equalizers	5
1.4 Motivation	7
1.5 Organization of the Thesis	8
CHAPTER-2: Literature Review	10
2.1 Classification of Battery Equalizers based on topology	10
2.1.1 Dissipative Circuits	10
2.1.2 Non-Dissipative Circuits	12
2.2 Classification based on Equalizer Control Variable	21
2.3 Research Gaps in existing converters	21
2.4 Research Objectives	22
CHAPTER-3: Architecture and Operating Principle of Proposed Voltage Equalizer	23
3.1 MMBE	23
3.1.1 MMBE Architecture	23

3.1.2 MMBE Operating Modes	25
3.2 MCBB	27
3.2.1 MCBB Architecture	27
3.2.2 MCBB Operating Modes	28
CHAPTER-4: Switching Algorithm	33
4.1 Motive of Switching Algorithm	33
4.2 Switching Algorithm logic and flow chart	33
CHAPTER-5: Control Strategy	36
5.1 Motive of Control Strategy	36
5.2 Dual Loop Current Control	36
CHAPTER-6: Performance Analysis	39
6.1 System Configuration	39
6.2 Cases Considered for Effectiveness of Equalizer MMBE	42
6.2.1 Case I	43
6.2.2 Case II	46
6.3 Cases Considered for Effectiveness of Equalizer MCBB	47
6.3.1 Case I	48
6.3.2 Case II	51
6.4 Comparison of Proposed Equalizer with other Equalizer based on number of components used	54
CHAPTER 7: CONCLUSION AND FUTURE SCOPE OF WORK	56
7.1 Conclusion	56
7.2 Future Scope of Work	57

REFERENCES

List of Figures

Fig. 1.1	Energy Outlook over contribution of various energy sources in INDIA (2020-2040)	3
Fig. 1.2	Wastage of energy and capacity during charging and discharging for an unbalanced battery pack connected in series.	7
Fig. 2.1	Fixed shunt resistor equalizer	11
Fig.2.2	Switched shunt resistor equalizer	11
Fig. 2.3	Switched capacitor equalizer	12
Fig. 2.4	Single switched capacitor equalizer	12
Fig. 2.5	Double-tiered switched capacitor equalizer	13
Fig. 2.6	Modularized switched capacitor equalizer	14
Fig. 2.7	Single inductor equalizer	15
Fig. 2.8	Coupled inductor equalizer	15
Fig. 2.9	Single winding transformer equalizer	16
Fig. 2.10	(a) Flyback Structure & (b) Forward Structure Multi winding transformer equalizer	16
Fig. 2.11	Single controlled switch multiple transformer equalizer	17
Fig. 2.12	Single switched capacitor modularized multi-winding transformer equalizer	18
Fig. 2.13	Buck-boost based voltage equalizers proposed by Yanqin Zhang [51]	19
Fig. 2.14	Buck-boost based voltage equalizers proposed by Shungang Xu [52]	19
Fig. 2.15	Buck-boost based voltage equalizers proposed by Nguyen-Nghia Do [53]	20
Fig. 2.16	Buck-boost based voltage equalizers proposed by XinBo Liu [54]	20
Fig. 2.17	Buck-boost based voltage equalizers proposed by Shun-Chung Wang [55]	24
Fig. 3.1	Schematic diagram of MMBE equalizer	25-26
Fig. 3.2	(a)-(d) operateing modes of MMBE	27
Fig 3.3	Architecture of MCBB equalizer	30-31
Fig. 3.4	(a)-(d) operateing modes of MCBB	35
Fig. 4.1	Switching Algorithm for enabling controller MOSFETs from controller	38
Fig. 5.1	Control strategy for MMBE and MCBB equalizers	43
Fig. 6.1	Voltage waveform for Case I in MMBE	44
Fig. 6.2	SOC waveform for case I in MMBE	44
Fig. 6.3	Inductor current waveform for case I in MMBE	45
Fig. 6.4	Voltage waveform for case I with delay for ensuring OCV	45
Fig. 6.5	SOC waveform for case I with delay	46

Fig. 6.6	SOC waveform for case II in MMBE	47
Fig. 6.7	Current waveform for case II in MMBE	49
Fig. 6.8	Real time voltage waveform for case I	49
Fig. 6.9	Inductor current waveform for case I	50
Fig. 6.10	SOC waveform for case I	50
Fig. 6.11	Voltage waveform for case II with delay for ensuring OCV	51
Fig. 6.12	SOC waveform for case I with delay	52
Fig. 6.13	Real time voltage waveform for case II	52
Fig. 6.14	Current waveform for case II	53
Fig. 6.15	SOC waveform for case II	54

List of Tables

Table 6.1. Converter and Battery Cell data	40
Table 6.2. Possible cases based on different soc levels of battery and its position in string	41
Table 6.3. Different Cases of battery SOC levels demonstrating parallel operation of PEL in MMBE	42
Table 6.4. SOC and Voltage relation for case I before starting equalization and after 0.5 sec of equalization	45
Table 6.5. Different Cases of battery SOC levels demonstrating parallel operation of PEL in MCBB	47
Table 6.6. Comparitive study of MMBE and MCBB with other equalizers	55

List of Abbreviations

STEPS	Stated Policies Scenario
SDS	Sustainable Development Scenario
HRES	Hybrid Renewable Energy Systems
SPV	Solar Photovoltaic
ESS	Energy Storage Systems
BESS	Battery Energy Storage Systems
PGCIL	Power Grid Corporation of India Limited
MNRE	Ministry of New and Renewable Energy
SOC	State-of-Charge
PWM	Pulse Width Modulation
AVDC	Adaptive Varied Duty Cycle
PEL	Parallel Equalizer Leg
MMBE	Multimode-Multilevel Bidirectional Equalizer
MCBB	Multi-looped Current-controlled Bidirectional Bridge

List of Symbols

B_n	Number of cells in string
PEL_l	PEL legs in equalizers
$M_{l_{High}}$	high side MOSFET of PEL_l
$M_{l_{Low}}$	low side MOSFET of PEL_l
D_l	Diode in auxiliary circuit of PEL_l
L_{Dl}	Inductor in auxiliary circuit of PEL_l
$Av_{l_{High}}$	average voltage for high side battery string
$Av_{l_{Low}}$	average voltage of low side battery string
V_{B_n}	Voltage of cell n in string
$E_{l_{High}}$	Enable for high side MOSFET
$E_{l_{Low}}$	Enable for low side MOSFET
i^*_{Ll}	reference current for current control
K_{Pv_H}	Proportional gain value for high side voltage controller
K_{Iv_H}	integral gain value for high side voltage controller
K_{Pv_L}	Proportional gain value for low side voltage controller
K_{Iv_L}	integral gain value for low side voltage controller
d'_{1H}	modulating signal for PWM in high side
d'_{1L}	modulating signal for PWM in low side
K_{Pi_H}	Proportional gain value for high side current controller
K_{Ii_H}	integral gain value for high side current controller
K_{Pi_L}	Proportional gain value for low side current controller
K_{Ii_L}	integral gain value for low side current controller

CHAPTER 1

INTRODUCTION

1.1 Need for Renewable Power Systems

Electricity is extremely important in today's society. In day-to-day operations, electricity is essential. Increased use and depletion of fossil resources have resulted in energy shortages, putting the globe in peril [1]. Electrical energy is the most practical source of energy since it can be turned into any other form. In terms of transmission, distribution, and control, it is one of the most adaptable kinds of energy.

With the world's growing energy need, renewable energy has become a difficult area to master. The scarcity of fossil fuels and worries about global warming caused by greenhouse gases are two motivating drivers for alternative and renewable energy research [2]. Because of their abundance and environmental friendliness, conventional sources are more sustainable [3]. Despite greater initial expenditure, a large number of governments, corporations, and organizations have begun commercial renewable energy-based power producing projects.

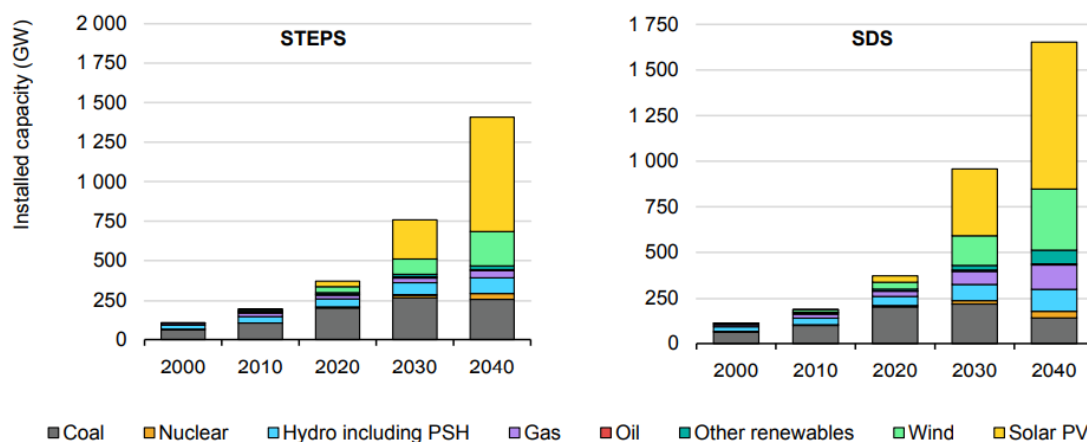
Despite the continuing of logistical issues and rising pricing, renewable power capacity additions set a new high in 2021, and biofuels demand nearly rebounded to pre-Covid levels. The Russian Federation's (hereafter "Russia") invasion of Ukraine, on the other hand, is sending shockwaves across energy and agriculture markets, culminating in a worldwide energy crisis unlike any other. Many governments are attempting to protect citizens from rising energy prices by

reducing reliance on Russian supply and proposing initiatives to hasten the transition to renewable energy technology.

According to IEA Renewable Energy Report – May 2022 Analysis [4], annual renewable capacity additions reached a new record in 2021, climbing 6% to about 295 GW, despite continuing pandemic-related supply chain issues, building delays, and record-high raw material prices. Due to rising commodity and freight prices, solar PV and wind costs are likely to stay higher in 2022 and 2023 than pre-pandemic levels. However, due to significantly greater rises in natural gas and coal prices, their competitiveness improves. Renewable capacity is predicted to grow by more than 8% in 2022, reaching about 320 GW. However, unless new rules are quickly enacted, growth will stay stable in 2023, since solar PV expansion will not be able to fully compensate for decreased hydropower and consistent year-over-year wind additions.

India is the world's third most energy-consuming country [5]. It has grown to be one of the world's greatest drivers of energy demand growth, and it has achieved tremendous progress toward its goal of universal electrification for residential users, with 100 million people receiving access in 2018. In India, the percentage of renewable energy used varies greatly by state. The solar and wind share of India's 10 renewables-rich states (Tamil Nadu, Karnataka, Gujarat, Rajasthan, Andhra Pradesh, Maharashtra, Madhya Pradesh, Telangana, Punjab, and Kerala) is much greater than the national average of 8.2%. In Karnataka, solar and wind power generate roughly 29% of yearly electricity, compared to 20% in Rajasthan, 18% in Tamil Nadu, and 14% in Gujarat (financial year [FY] 2020/21). India's renewable-rich states already have a greater percentage of variable renewable energy (VRE) than most other countries [6]. As a result, several state governments are already experiencing problems with system integration.

The evolution of India's electricity capacity mix in the Stated Policies Scenario and the Sustainable Development Scenario, 2000-2040



IEA. All rights reserved.

Source: IEA [India Energy Outlook 2021](#).

Fig. 1.1 Energy Outlook over contribution of various energy sources in INDIA (2020-2040)

India's potential routes to 2030 and 2040 are examined in the IEA World Energy Outlook 2021 scenarios. In Fig. 1.1, the Stated Policies Scenario (STEPS) depicts a roadmap for India to reach its nationally decided contribution under the Paris Agreement based on current policies and proclaimed policy intentions. With a decreased percentage of coal, the Sustainable Development Scenario (SDS) contains significant technical possibilities for more sustainable development. Solar and wind power will surpass coal power capacity of 269 GW in 2030, according to the STEPS. By 2040, the WEO estimates that the STEPS will have over 620 GW of solar and 219 GW of wind capacity, while the SDS will have over 720 GW of solar and 309 GW of wind. Coal capacity grows until 2030 in all scenarios before declining. Coal is projected to reach 260 GW in the STEPS by 2040, but only 144 GW in the SDS.

There are various methods for India to meet its renewable energy objectives, but they all have one thing in common: a high amount of solar and wind energy. As a result, greater power system flexibility is required. Hybrid renewable systems are being proposed as a possible approach to address the intermittency and unpredictability of renewable systems. Hybrid Renewable Energy Systems (HRES) combine one or more renewable energy sources with or without storage options to provide flexible and cost-effective power systems that may operate

independently or in conjunction with the grid. Wind-PV systems are the most extensively installed and managed because wind and solar energy are complimentary in nature. However, when linked to the electric grid, such renewable energy technologies encounter several challenges. The following are the key points raised:

- The electricity generated is intermittent, due to the uncontrolled nature of energy sources like wind and solar.
- The system is unreliable, despite the fact that it uses strict forecasting procedures and measurements.
- Grid stability and system integrity are impacted by power fluctuations.
- Power availability and peak demand times are out of sync.
- Inadequate transmission and distribution infrastructure prevents the generated green electricity from being evacuated.

Consumers would benefit greatly if they can purchase electricity directly from renewable sources. Alternatively, conventional energy supply might be integrated with renewable energy, with batteries and generators serving as backup in remote regions. In the lack of renewable energy, the grid will step in to help, and vice versa.

A robust grid interface is needed to filter out fluctuations in renewable energy sources and offer users with reliable electricity. Most solar photovoltaic (SPV) systems are grid-connected. As a result, to feed the grid without any fluctuations, a consistent grid interface is necessary. DC voltage is provided by solar PV cells. Converters convert DC electricity into AC electricity.

1.2 Importance of Battery Energy Storage Systems (ESS)

The majority of the problems with renewable energy systems may be solved by providing a storage facility, which, when properly designed and run, will make the power system very stable and dispatchable. Seasonal changes and insufficient power from wind turbines further complicate the integration of various sources, necessitating storage facility adaptation. Many European countries, such as Germany, have already begun to use large-scale energy storage in conjunction with renewable energy initiatives. However, in India, energy storage is still not taken

seriously, with numerous myths and misunderstandings clouding the power industry. India has a massive electricity shortage in many rural regions, with power outages lasting up to 16 hours every day. The majority of power industry investment is concentrated on the building of transmission infrastructure and the laying of power lines. In the last decade, these issues have hampered storage expansion. With the rising penetration of renewable systems in the grid, however, the necessity to plan ahead for storage solutions has become critical.

Battery UPS systems have been installed at a home level across the country for storing grid power in recent years, but such systems have not been deployed for PV or other renewable systems. For decades, large-scale hydro storage has been the sole method of storage used in the country [7]. This scenario is about to undergo a big adjustment to meet the issue of increased wind and PV system deployment.

According to the Green Corridor Report by Power Grid Corporation of India Limited (PGCIL), the anticipated storage capacity required by 2020 to meet the specified renewable energy objectives is 5 GW. Provisions are gradually being developed to promote storage usage. Ministry of New and Renewable Energy (MNRE) has increased subsidies for PV systems with energy storage via the Jawaharlal Nehru National Solar Mission. However, these measures pale in contrast to the efforts required to accomplish the energy storage goals. As a result, Indian Power policymakers need to design regulations that stimulate the manufacture and deployment of energy storage, therefore aiding the renewable energy milestones.

It's high time to consider alternate energy storage methods that can be used with stand-alone renewable systems. Many energy storage firms, such as AES and Panasonic, are eyeing India for large-scale storage implementation. Energy storage markets are set to heat up as a result of intensive discussions on establishing microgrids to electrify the country's communities. As a result, research and studies on energy storage devices are critical and must be implemented immediately.

1.3 Requirement of Battery Equalizers

To satisfy the needs of high voltage and/or high power, Energy Storage Systems (ESS) use series-connected batteries. Battery protection, battery

management, and battery equalization are all features that a high-end battery energy storage system should have. The battery equalization, in particular, has a significant impact on battery life.

To deliver the appropriate system voltage and power, cells are frequently connected in series to form a battery bank as individual cells have low terminal voltage. Individual battery cell imbalance in a battery bank is a regular occurrence. State-of-Charge (SOC) variations across cells are a well-known imbalance. Intrinsic and extrinsic variations between battery cells generate this imbalance. The biggest contribution to inherent variances is diversity in manufacturing procedures. There may be modest changes in internal resistances between two batteries/cells from the same manufacturer with identical specs. Internal resistance and internal battery capacitance are dependent on the chemical makeup of the internal battery, hence It's extremely unlikely to create two cells with identical properties. Cell performance varies due to differences in capacity, self-discharge rates, and internal resistances. External circuitry and temperature influence are examples of extrinsic factors. Uneven temperature distribution in a battery bank has an impact on cell properties and results in performance variations. Although higher operating temperatures boost capacity and output, they also hasten the ageing of battery cells. Lowering the operating temperature reduces performance. The external circuitry attached to each cell for sensing, control, and protection is the other extrinsic distinction. These circuits use varying amounts of power from each battery cell, worsening the imbalance. Several discharge cycles can also deteriorate the electrolyte of a battery and change its internal resistance over time. These changes are unique to each battery/cell, and as a result, cells linked in series develop various internal properties over time.

Energy loss in the battery bank is the most significant effect of cell imbalance [8]. Because of the aforementioned variances across cells, each cell's energy usage varies. This results in disparities in SOC between cells. The performance of the entire battery bank will be limited by cells with the lowest and highest SOC. Overcharging or over-discharging would pose a safety risk to the battery bank. The voltage differential will widen if you use an unbalanced battery pack. Because the cells in series will have the same charging and discharging

current, their rate of charge and discharge will vary due to their differing internal properties, resulting in a voltage imbalance in the battery. The cell with the lowest SOC will approach the lower limit of safe operating voltage first when discharging, requiring the BMS to cut off the operation. During charging, a similar situation occurs: the cell with the highest SOC will reach the upper limit of safe operating voltage first, forcing the BMS to terminate the charging process. As a result, some of the other cells' energy and capacity is squandered. which will eventually damage the battery cells and reduce battery life. The cell with the least energy capacity among the pack limits the total battery pack capacity when in operation. Fig. 1.2 depicts the energy and capacity losses in an imbalanced condition.

Battery Equalizing circuits efficiently minimize the voltage difference between the cells, providing optimal energy and extending the battery's lifespan.

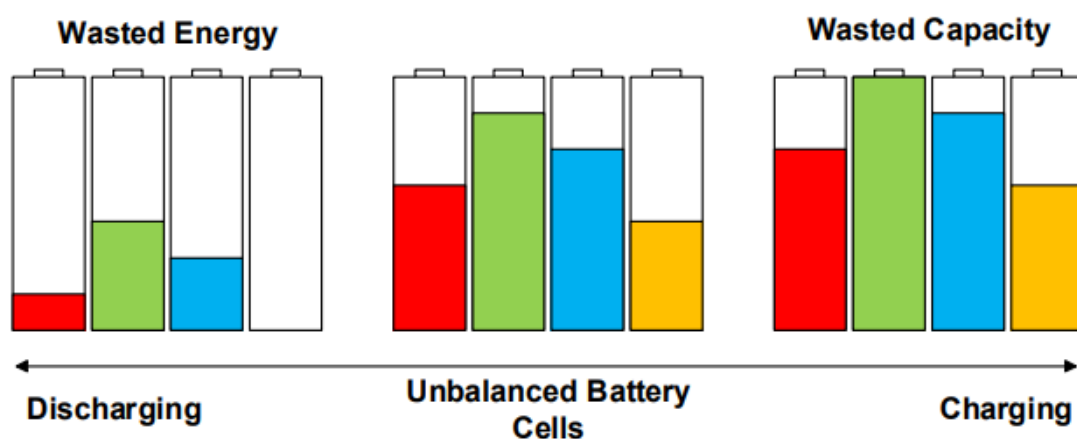


Fig. 1.2 Wastage of energy and capacity during charging and discharging for an unbalanced battery pack connected in series.

1.4 Motivation

This research work mainly focuses on developing a novel battery voltage equalizer for effective battery balancing. The primary function of the battery equalizer is to monitor and regulate the internal cell voltages and capacities at same level for all the cells in a string. Through- out the years, the researchers have developed several topologies for battery voltage equalizer with different level of accuracy and complexity to balance the cells in a string, which is elaborated in chapter 2. From the review of related research work, it could be concluded that the existing equalizer topologies needs some improvement for a more hardware efficient topology, faster and targeted battery balancing equalizer.

- To achieve Faster Battery balancing
- Achieving targeted battery balancing (energy could be transferred from any cell to any cell in the string to achieve balancing.)
- Hardware compliant topology (use of fewer number for passive elements, high and low side switches, respective gate drivers, and voltage sensors)

1.5 Organization of the Thesis

As stated previously, the primary goal of the thesis is to develop a battery voltage equalization, which involves a thorough examination of the architecture and modes of the proposed topology, switching mechanism, and control strategy. The thesis is organized as follows:

Chapter 1 This chapter provides the reader with an introduction of Renewable energy scenario and background on the importance of battery-based energy storage systems and the need for a battery voltage equalizer to improve the battery pack performance and life time.

Chapter 2 This chapter elaborates on the literature necessary to develop an insight of the topic, a brief outline of the development in battery equalizer and understand the research gaps in existing voltage equalizers.

Chapter 3 This chapter includes the detailed architectural study of the proposed topology along with the operating modes. It also compares the topology with other equalizers mentioned in the literature review in order to emphasize its key benefits.

Chapter 4 The logic for the switching algorithm is explained in this chapter using a flow chart and mathematical equations. The switching algorithm is used to enable the control strategy of each MOSFET, which is delt in next chapter.

Chapter 5 This chapter deals with the control strategy used for triggering the pulses in order to transfer the energy from higher voltage cell to a lower voltage cell, thus balancing the battery sting. The control strategy uses dual loop control,

the outer loop being the voltage loop and inner loop being the current controlled loop.

Chapter 6 This chapter validates the efficacy of the proposed equalizer. Two different cases are considered and the results are presented that support the effective performance of the proposed equalizer.

Chapter 7 This chapter summaries the contributions of this thesis and highlights potential future research opportunities.

CHAPTER 2

PROPOSED HYBRID SYSTEM

2.1 Classification of Battery Equalizers based on topology

Cell voltage equalisation is a hotly debated scientific issue these days. As a result, several research have been done in order to develop and enhance cell equalisers. Existing cell equalisers are classified into two types depending on the components utilised to equalise cell voltages, namely dissipative and non-dissipative circuits. This section includes a brief overview of the various types of cell equalisers as well as a circuit schematic.

2.1.1 Dissipative Circuits

Resistors are used in dissipative circuits to equalise cell voltages. Due to the usage of resistors in parallel with each cell, these equalisers are also known as shunting resistor equalisers. They may also be divided into two types based on the control method of the equaliser, namely fixed shunting and switched shunting resistor equalisers. These equalisers are basic and have various advantages such as compact size, low cost, simple control, and quick installation. The principal drawbacks of these equalisers are large energy losses and heating issues.

- Fixed shunt resistor cell equalizer

Passive equalisers, often known as shunt resistor cell equalisers, are a simple equalisation approach. They are low-cost, small-size equalisers that are simple to integrate into battery systems. The shunt resistor removes extra energy from the high-voltage cell in the form of heat [9-15]. As a result, this equaliser has a significant energy loss and a heat management difficulty.

A fixed resistor is linked in parallel with each battery cell in fixed shunting resistor equalisers as shown in Fig. 2.1. Because of the unneeded external control system, the control method of this equaliser is straightforward. Because the amount of current consumed by the shunt resistor is proportional to the cell voltage, increasing current is given to the shunt resistor as the cell voltage increases. This procedure discharges the high-voltage cells until they are all balanced. The shunt resistor's current draw, on the other hand, is uncontrolled. As a result, cell voltages are not completely controlled.

- Switched shunt resistor cell equalizer

The switched shunt resistor cell equaliser is a shunt resistor equaliser with control switches as depicted in Fig. 2.2. A switch is linked in series with each shunt resistor that is connected in parallel with the relevant cells. This topology supports two modes of operation. The first is basic control mode, which controls all switches with a single on/off signal. During this operation, the entire resistor is connected or unplugged from the relevant cell at the same time [16-17]. Another option is detecting mode, in which the voltage of each cell is continually checked. When imbalanced circumstances are detected, the switch determines which resistors should be connected to which cells. Instead of connecting all cells, this technique connects just selected and necessary cells for a certain period of time. This equalisation approach outperforms the fixed resistor strategy.

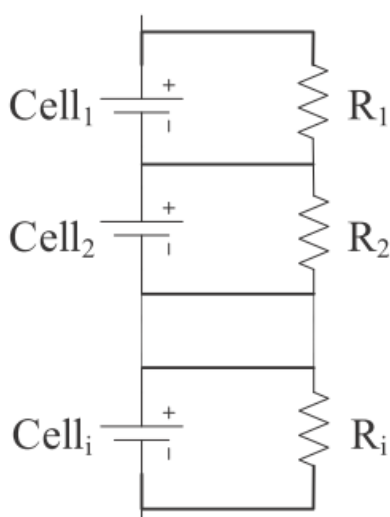


Fig. 2.1 Fixed shunt resistor equalizer

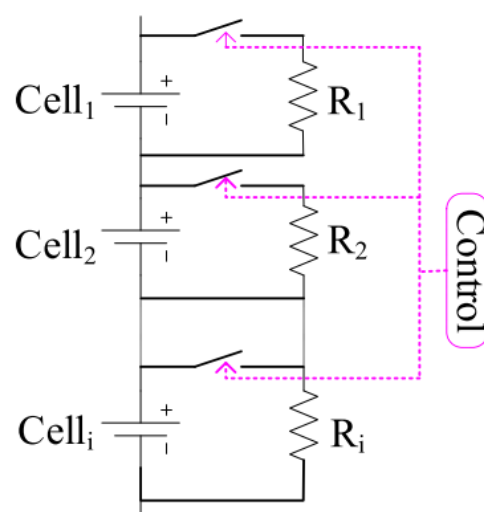


Fig.2.2 Switched shunt resistor equalizer.

2.1.2 Non-Dissipative Circuits

Capacitors and inductors are used in active equalisers to equalise cell voltages as they can store and transport energy. These components transmit surplus energy from high voltage cells to low voltage cells until all cell voltages are balanced. Various converters are also employed to equalise cell voltage. Active cell equalisers are classified into three types depending on their principal charge transferring components: capacitor, inductor or transformer, and converter-based.

- Capacitor based cell equalizer

Cell equalisers based on capacitors are used to transfer energy between cells and packs by storing energy in capacitors for some intermediate time externally. The switching control is achieved automatically by measuring the cell voltages. Nonetheless, they are affected by large current ripples. Capacitor based cell equalizers are classified as switched capacitor, single switched capacitor, or two tiered switched capacitor.

Although switched capacitors are simple to create and regulate, equalisation takes a long time. Fig. 2.3 depicts the switched capacitor cell equaliser, which has i cells and $i-1$ capacitors and allows the cells to be charged or discharged. Using a simple control method, the single switched capacitor cell equalisation selects a higher and a lower cell to transfer the surplus energy of the higher cell to the lower cell [20-23]. The single switched capacitor cell equalisation (shown in Fig. 2.4) includes a single capacitor and a number of switches to equalise the charge levels of the cells.

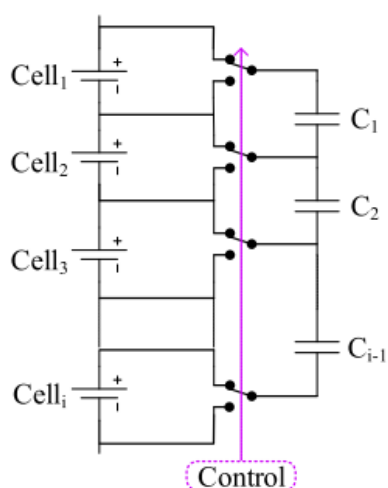


Fig. 2.3 Switched capacitor equalizer

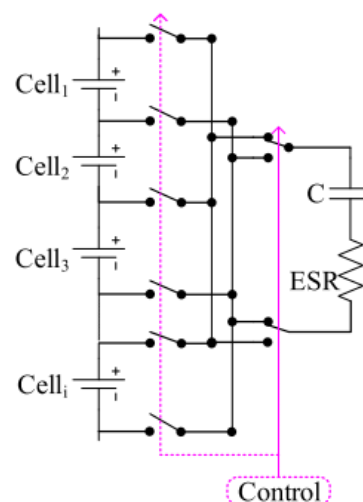


Fig. 2.4 Single switched capacitor equalizer

As illustrated in Fig. 2.5, a derivation of the switched capacitor is employed in the double-tiered switched capacitor cell equalisation, which uses two capacitor tiers to

transmit cell energy [24,25]. It employs a double-tiered capacitor to cut equalisation time in half, particularly compared to the switched capacitor cell equalizer.

The modularized switched-capacitor-based equalisation technology has a significant influence on increasing equalisation performance while maintaining acceptable balance [26-28]. As illustrated in Fig. 2.6, the modularized system considers controlling the battery pack in some modules for charge balancing. Each module of the battery pack is equipped with a switched-capacitor-based equalisation system and is linked to the master equalisation controller of a single switched capacitor, allowing for quick equalisation within the pack and modules and minimal voltage and current demands on switches.

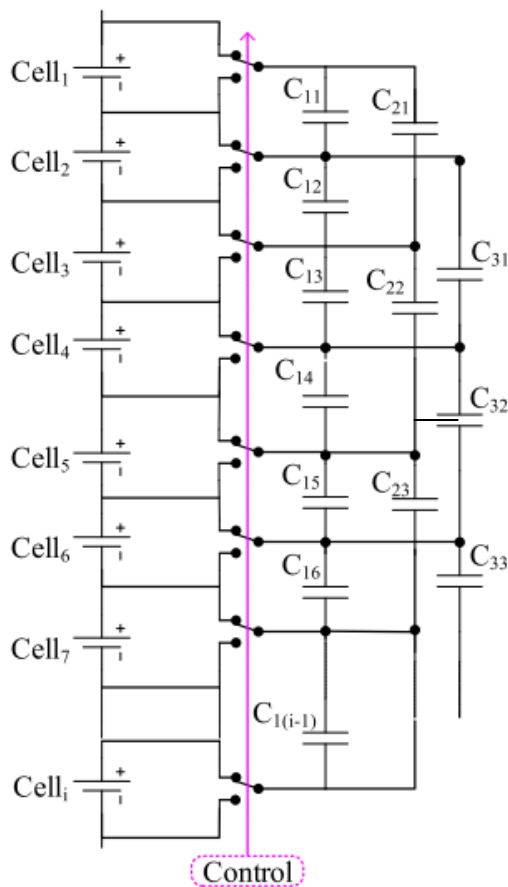


Fig. 2.5 Double-tiered switched capacitor equalizer

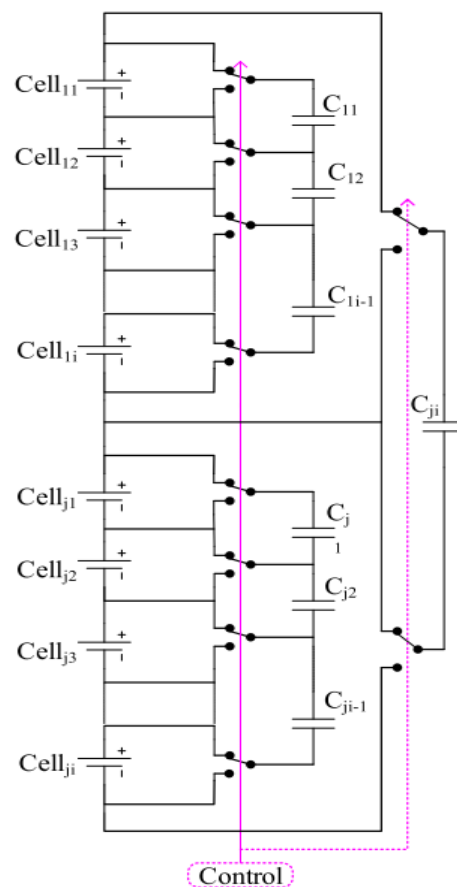


Fig. 2.6 Modularized switched capacitor equalizer

Capacitor-based balancing employs switched capacitor cells, delta structures, star structures, chain structures, and coupled capacitors and has the benefit of not requiring

voltage sensors; nevertheless, uncontrolled balancing currents and longer balancing times are significant drawbacks.

- Inductor/Transformer based cell equalizer

Inductor/transformer-based cell equalisers are charge equalisation systems that use inductors or transformers to transmit greater energy from a cell, module, or pack to another cell, module, or pack. Because of the high equalisation current employed in these equalisers, they usually require a shorter equalisation time. They have several topology variants, like single inductor, coupled inductor, single winding transformer, multi-winding transformer, multiple transformers and modularized transformer-based cell equalizer.

The single inductor cell equalisation depicted in Fig. 2.7 transfers energy from a higher energy cell to a lower energy cell using a single inductor. It detects and monitors the voltage levels of each cell and picks two cells for energy exchange through switching inductor. It is less expensive and takes less time to equalise.

The coupled inductor-based cell equalisation (shown in Fig. 2.8) analyses the voltage levels of the neighbouring battery cells and switches the higher energy cell first by delivering a pulse width modulation (PWM) signal to MOSFET switches to transfer the energy to the lower energy cell in the entire pack [29,30]. Due of the passage of energy from the higher cell to the final cell in a big battery pack, the equalisation period of this cell equaliser is longer than that of a single inductor CEC.

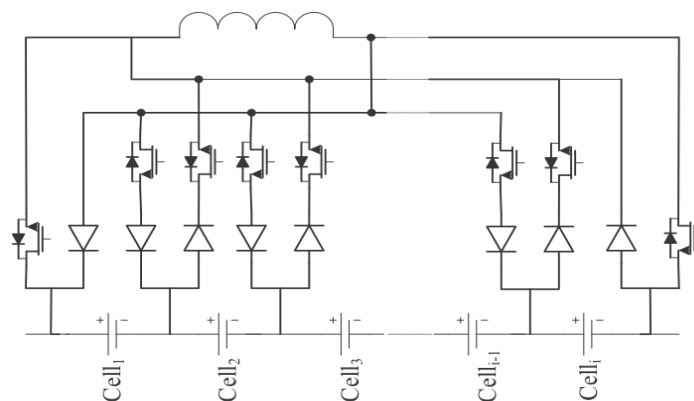


Fig. 2.7 Single inductor equalizer

As shown in Fig. 2.9, the single winding transformer cell equalisation employs the switched capacitor cell equaliser structure [31,32]. It is also known as a switched transformer cell equaliser because it allows equalisation current to flow through the transformer to transfer energy from the cell pack to the lower energy cell or from the higher cell to the cell pack by regulating the switches. Because of the numerous switches and transformers, this configuration is highly costly.

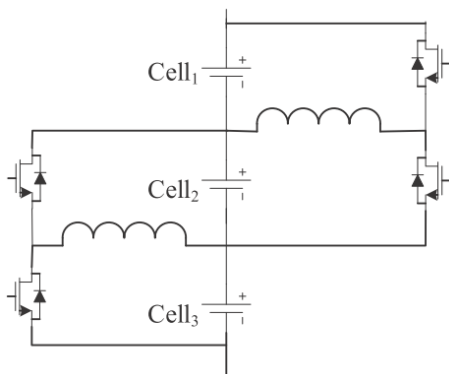


Fig. 2.8 Coupled inductor equalizer

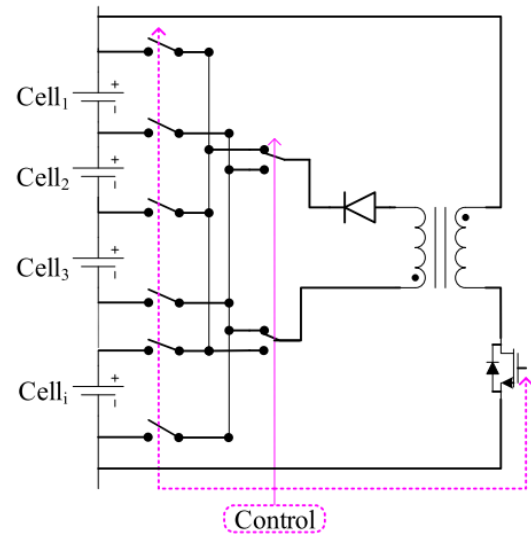


Fig. 2.9 Single winding transformer equalizer

The multi-windings transformer cell equaliser employs a single core transformer with a main winding and numerous secondary windings to accommodate each battery cell in each secondary winding [33,32]. It is a shared transformer-based cell equalisation that distributes stored energy from the primary to the identified lower energy cell in the secondary of the transformer to transfer energy similar to the flyback structure as illustrated in Fig. 2.10. (a). It can be configured similarly to the forward arrangement shown in Fig. 2.10 (b), with each secondary in series with a MOSFET switch and an anti-parallel diode, and the primary with a forward diode to transmit energy from the higher energy cell to the pack through a transformer. This cell equaliser is good; nevertheless, it is expensive and hard to develop; and it suffers from saturation.

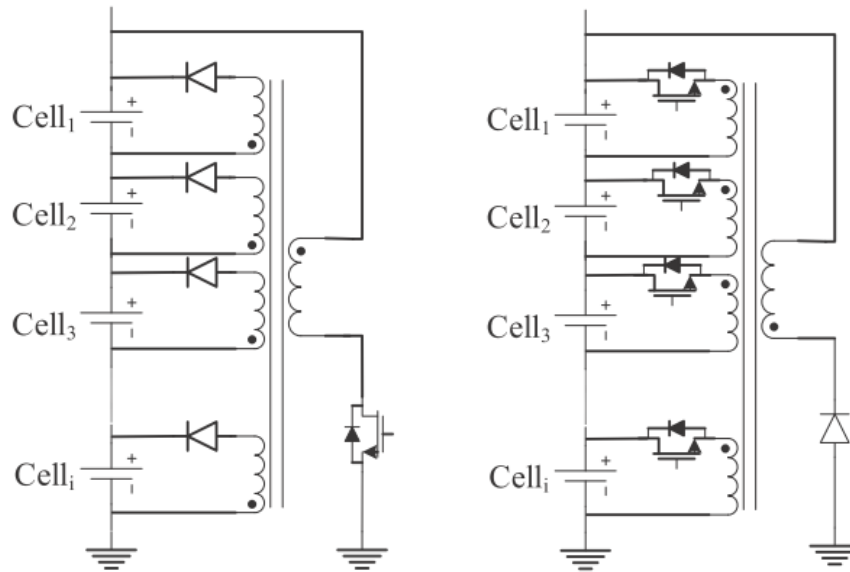


Fig. 2.10 (a) Flyback Structure

Fig. 2.10 (b) Forward Structure

Multi winding transformer equalizer

The multiple transformer cell equalisation uses a specialised transformer for each battery cell separately [35-37]. It connects in a common place at primary side with a single controlled switch, as shown in Fig. 2.11. It works similarly to a single winding transformer cell equalisation except that the switches are replaced with a transformer for each battery cell to transfer surplus energy from the higher energy cell to the lower energy cell in the pack through a PWM controlled transformer. The design may be adjusted for a big pack or modular design, but it is heavy and costly, and it includes magnetising losses owing to the usage of numerous transformers.

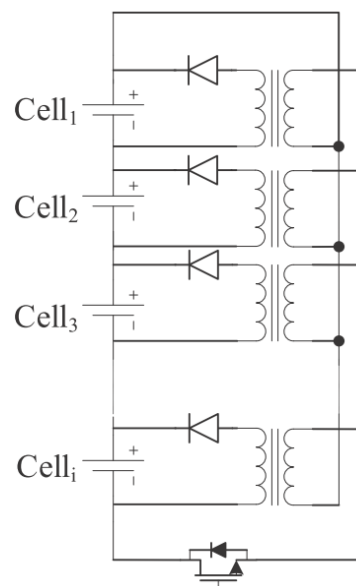


Fig. 2.11 Single controlled switch multiple transformer equalizer

The modularized multi-windings transformer-based cell equaliser, shown in Fig. 2.12, is more efficient and reliable configurations for the battery cell equaliser [37,39]. It depicts a modularized multi-winding transformer with a single switched capacitor cell equaliser, in which the whole battery pack is separated into modules, each of which is controlled by a separate multi-winding transformer cell equaliser. It converts energy from the higher energy cell to the module and then transports the energy to another module or pack via switched capacitor.

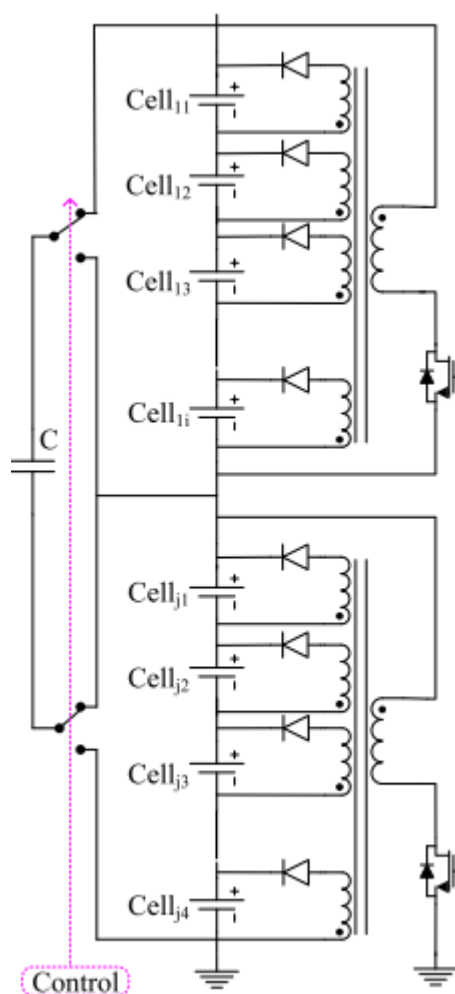


Fig. 2.12 Single switched capacitor modularized multi-winding transformer equalizer

- Converter based cell equalizer

Power converters are used in converter-based cell equalisers to redistribute surplus energy from high voltage cells to low voltage cells. To equalise cell voltages, a sufficient number of converters have been added. Converter equalisers are classified into several types according on the type of converter utilised, including Cuk, fly-back, ramp, full-bridge, buck/boost, and quasi-resonant converter equalisers [40-50]. These cell

equalizers provide efficient characteristics and total control over the equalization process, but the design and implementation are relatively expensive and complex. The intelligent control technique uses a PWM signal to regulate the switching. Among these buck-boost based cell equalizers are the hot topic as they are non-isolated and require lesser number of passive elements.

Of all the converter based equalizers, buck-boost based circuitry has several balancing topologies [56-60]. Among them a majority uses sequential equalization techniques, while some topologies uses parallel structure of buck-boost arranged across the battery string.

In [51], Yanqin Zhang has presented a modularized buck-boost topology. The topology takes two adjacent cells as a module and sets balancing converter between modules. Thus, it can realize bidirectional balancing current travelling between neighboring modules so as to achieve the bidirectional balance between non-adjacent cells of the lithium-ion battery pack.

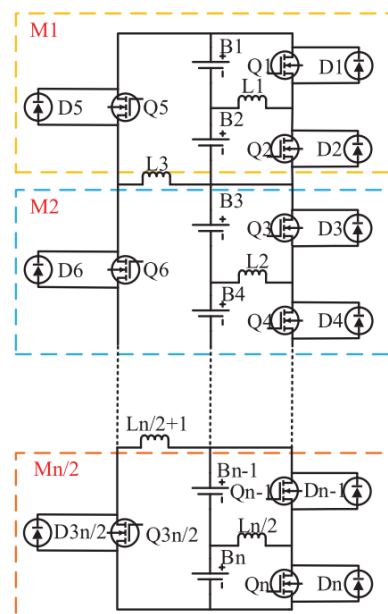


Fig. 2.13 Buck-boost based voltage equalizers proposed by Yanqin Zhang [51]

In [52], Shungang Xu has presented a cascaded equalizer for two layer energy transfer. There are different modes of operation based on whether the maximum voltage cell is located at the top of the whole battery string or in the middle of the battery

string. The placement of inductors plays a crucial role in determining the speed of the equalizer.

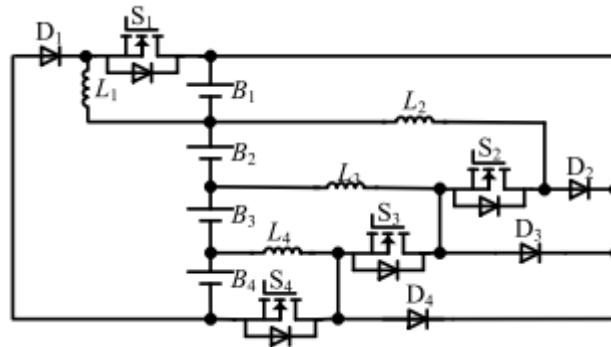


Fig. 2.14 Buck-boost based voltage equalizers proposed by Shungang Xu [52]

In [53], Nguyen-Nghia Do has presented a parallel based topology for faster energy transfer from one or many higher-voltage cells to other cell(s). It achieves equalization in two cases, (i) end cell to the remaining cell equalization (ii) cell to cell equalization. It is able to achieve partial targeted balancing.

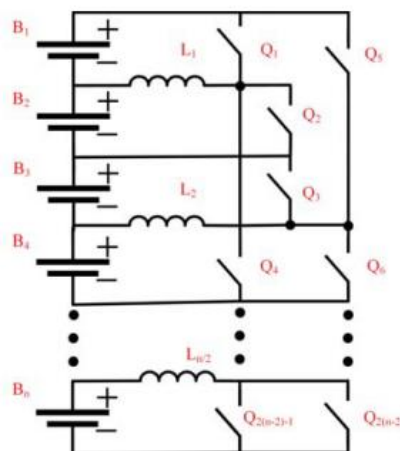


Fig. 2.15 Buck-boost based voltage equalizers proposed by Nguyen-Nghia Do [53]

In [54], XinBo Liu has presented similar circuitry with large current equalization strategy. Except for the first and last batteries, each battery has a route made up of two equalisation inductors, a completely controlled switch, and a battery. The equalisation inductors in the adjacent batteries are the same.

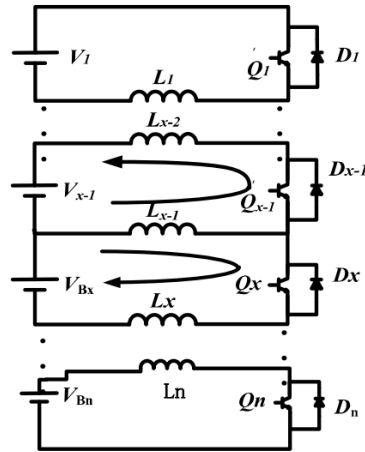


Fig. 2.16 Buck-boost based voltage equalizers proposed by XinBo Liu [54]

For all above topologies, there are a lot of high side mosfets used and thus a lot of high side isolated gate drivers and auxiliary supplies. Thus we need a better hardware compliant topology.

In [55], Shun-Chung Wang has presented a multilevel buck-boost topology, in which buck-boost configuration are such that the converter legs are parallel to battery string and to each other. Mixed integration of all power switches with gate drivers and auxiliary supplies is achievable since all converter legs are linked to the same battery pack. All low side mosfets are on same potential and can be connected to a corresponding single low side driver and isolation transformer making the circuit compliant, compact and inexpensive.

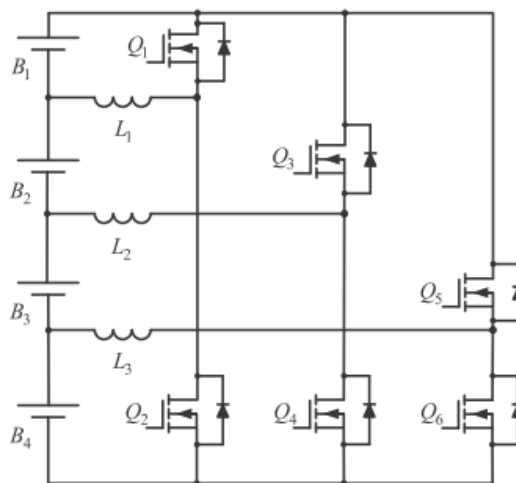


Fig. 2.17 Buck-boost based voltage equalizers proposed by Shun-Chung Wang [55]

2.2 Classification based on Equalizer Control Variable

Apart from equalizer topology, equalizer control algorithm also plays a vital role in deciding conversion efficiency of equalizer circuit and balancing speed. According to control variable used, it is generally classified into voltage-based, SOC-based and capacity-based algorithms. There are several BES that uses same variable but completely different algorithm flow from each other. Voltage based algorithms are easy to implement as voltage can easily be measured using sensors. SOC based algorithm is similar in approach but uses SOC value of cells which is estimated using voltage, current and temperature of cells, adding to the computational complexity of BES. Capacity-based algorithm determines charge in each cell by integrating current over the time and then calculating equalization charge that needs to be additionally added or removed from each cell to achieve complete equalization.

2.3 Research Gaps in Existing Converters

Based on the detailed study, it is evident to use converter-based equalization circuit with voltage-based algorithm of optimum and efficient balancing. Topology in [55] is favorable as it provides bidirectional energy flow and utilizes lesser number of high side MOSFETs, gate drivers and isolated power supplies. However, the equalization is slow as only one leg is operated at a time which doesn't ensure targeted battery balancing and needs major alterations for cases where battery voltages are neither occurring in ascending or descending order but randomly occurring such that lowest or highest voltage cells are found anywhere in middle of the string, thus requiring targeted battery equalization.

All the studied topologies are sequential, cascaded, or in parallel connection with the cell equalizer. They require a lot of high side MOSFETs which further require same number of isolated high side gate drivers and auxiliary supplies. After a detailed study, topology presented by Shun-Chung Wang [55] uses lesser high side MOSFETs and is more hardware compliant. The balancing algorithm adapted is adaptive varied duty cycle (AVDC) in which one Parallel Equalizer Leg (PEL) is operated based on maximum voltage difference between the parts of the battery pack connected on both sides of the inductor of that PEL. The operation of all other PEL is disabled. Also, duty cycle is calculated based on voltages of the cell and a constant theoretical current value. No actual current control mechanism is considered for the current across the inductor.

2.4 Research Objective

Two new topologies are proposed modified from [55] topology presented by Shun-Chung Wang. Following objectives are achieved after modification.

- The topology is hardware compliant. It uses lesser number high side MOSFETs, isolated gate drivers, auxiliary supplies. Also lesser number other components are used when compared to other topologies.
- Faster battery equalization
- Targeted energy transfer from higher energy cell to lower energy cell irrespective of the position in the string.
- Balancing current can be controlled to regulate the speed of balancing.
- Parallel balancing path to achieve targeted and faster balancing.

A modified Multimode-Multilevel Bidirectional Equalizer (MMBE) and Multi-looped Current-controlled Bidirectional Bridge converter (MCBB) is proposed which uses voltage as control variable for achieving targeted balancing and faster equilibrium by operating all the parallel legs at a time. The switching strategy adopted for each leg is done by grouping the battery string into two parts: high-side string and low side string, divided at the point of common coupling between the battery string and operating PEL. Each leg can transfer energy from one part of the string to other part, thus achieving targeted balancing by simultaneously operating all the legs without circulating currents. Each leg is operated based on a new simplified switching technique along with dual loop current control that offers advantage of designing the MMBE and MCBB equalizer for any required balancing current thus ensuring faster balancing. Moreover, MMBE and MCBB doesn't require separate voltage sensors for each battery as a single quad op-amp can be used with differential circuit along with ground referred voltage divider which makes the equalizer compact and affordable.

Both the equalizers are divided into following three parts. Each of these parts are dealt in detail in the subsequent chapters.

- (i) Power Circuit
- (ii) Switching Mechanism
- (iii) Control Circuit.

CHAPTER 3

ARCHITECTURE AND OPERATING PRINCIPLE OF PROPOSED VOLTAGE EQUALIZER

Detailed architectural study of two proposed topologies MMBE and MCBB are presented in this chapter along with its operating modes.

3.1 MMBE

3.1.1 MMBE Architecture

This topology can be adapted to any number of series connected battery string. Fig. 3.1 shows the schematic of the proposed MMBE power circuit. For the battery string having N number of cells in series (B_n : $n=1,2,3\dots N$), will be N-1 Parallel Equalizer Legs (PEL_l : $l=1,2,3\dots N-1$). Each PEL is composed of two MOSFETs, (M_{lHigh} : high side MOSFETs and M_{lLow} : ground referred low side MOSFETs), coupled inductors (L_{P_l} and L_{D_l}) and diodes (D_l) to invoke bidirectional buck-boost topology to enable energy flow in either direction such that overcharged cells should only transfer their energy to undercharged cells in a battery string as shown in Fig. 3.1. The diodes (D_l) in series with inductor (L_{D_l}) connected across a particular battery cell forms an auxiliary circuit to protect undesired discharging also aids faster battery balancing and ceases circulating currents due to multiple PEL operating simultaneously, besides acting as snubber circuit for the MOSFETs to ease out voltage stress across it.

Multiple PEL operates in parallel such that it can equalize the entire battery string directionalizing the flow of energy to the targeted battery cell(s). Each PEL operates independently to achieve targeted battery balancing and divides the entire battery string into two parts at the point of coupling as high side string and low side string (ground

referred). Only one MOSFET in each PEL will operate at a time to avoid short-circuiting of the battery string. If the average voltage for high side battery string ($Av_{l_{High}}$) has higher value than the average voltage of low side battery string ($Av_{l_{Low}}$), then $M_{l_{High}}$ is operated. Whereas if $Av_{l_{Low}}$ is higher than $Av_{l_{High}}$, then $M_{l_{Low}}$ is operated. Thus, equilibrium is achieved between the two parts of the string. In a similar way all the PELs operate in order to achieve redistribution of energy to form equilibrium in the entire string.

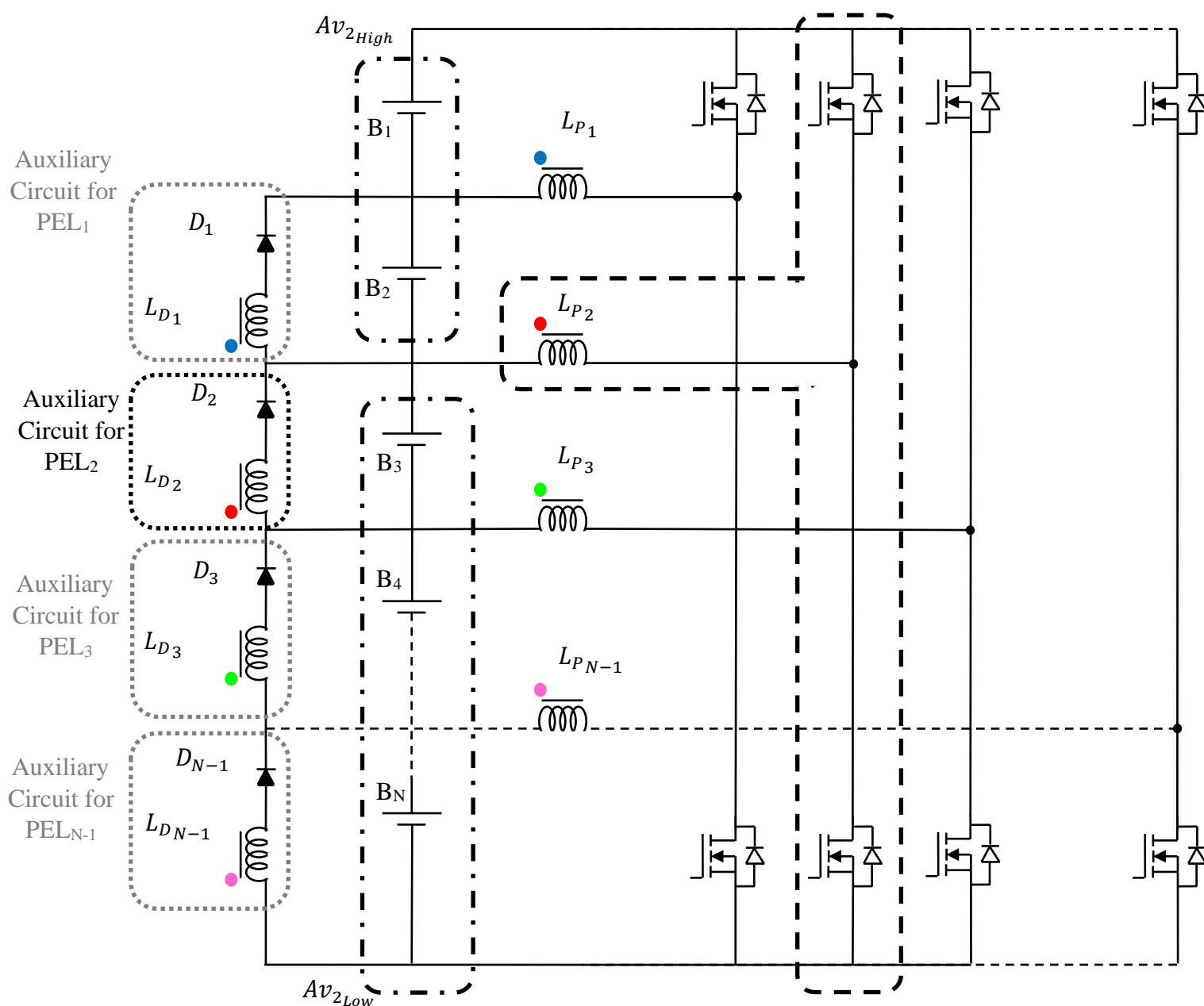


Fig. 3.1 Schematic diagram of MMBE equalizer

3.1.2 MMBE Operating Modes.

Fig. 3.2 (a) to 3.2 (d) presents the energy flow through a PEL_l when $M_{l_{High}}$ or $M_{l_{Low}}$ is operated. For the case when $M_{l_{High}}$ is operated, batteries in high side string ($\sum_{n=1}^l B_n$) gets discharged and accumulates their energy to L_{P_l} during T_{on} of duty cycle shown in Fig. 3.2(a). During T_{off} time of duty cycle, the stored energy in L_{P_l} is released and transferred to batteries on low side of the string ($\sum_{n=l}^{N-1} B_n$) through the body diode of $M_{l_{Low}}$ shown in Fig. 3.2(b). The auxiliary circuit aids the equilibrium process and transfers the energy to the targeted cell B_{l+1} . L_{D_l} and L_{P_l} are differentially such that it transfers energy only in one direction and the diode D_l connected in series with L_{D_l} blocks the reverse flow of energy. For the case when $M_{l_{Low}}$ operates, batteries on low side string ($\sum_{n=l}^{N-1} B_n$) gets discharged and stores its energy in L_{P_l} during T_{on} and during T_{off} the stored energy is transferred to high side group of batteries ($\sum_{n=1}^l B_n$) as shown in Fig. 3.2(c) and 3.2(d). In this case energy flow through auxiliary circuit is blocked by D_l diode.

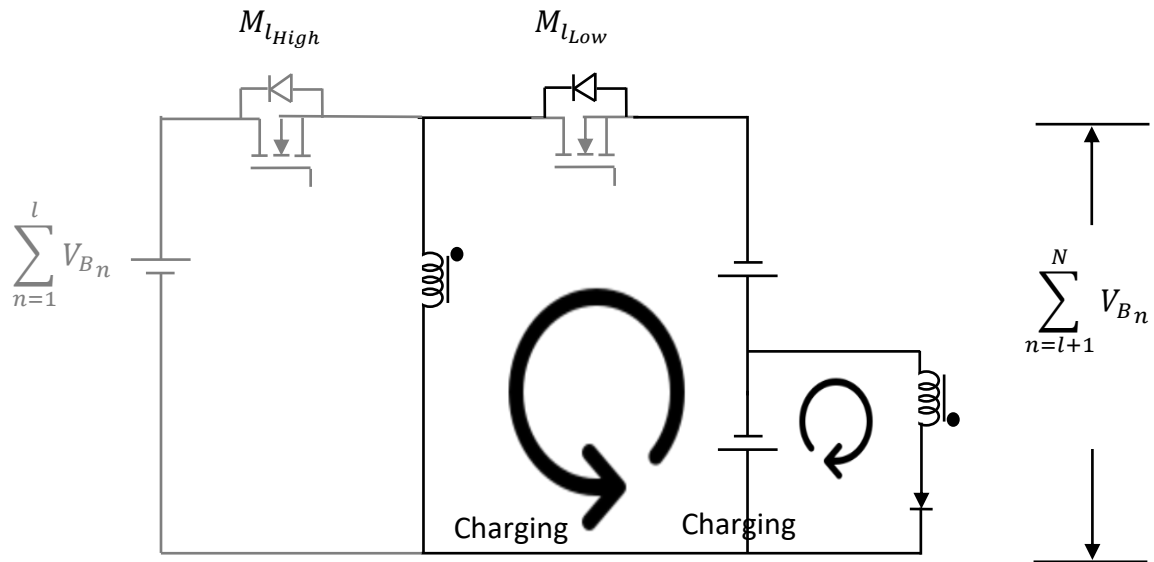


Fig. 3.2 (a) Energy flow for high side MOSFET operation during T_{on}

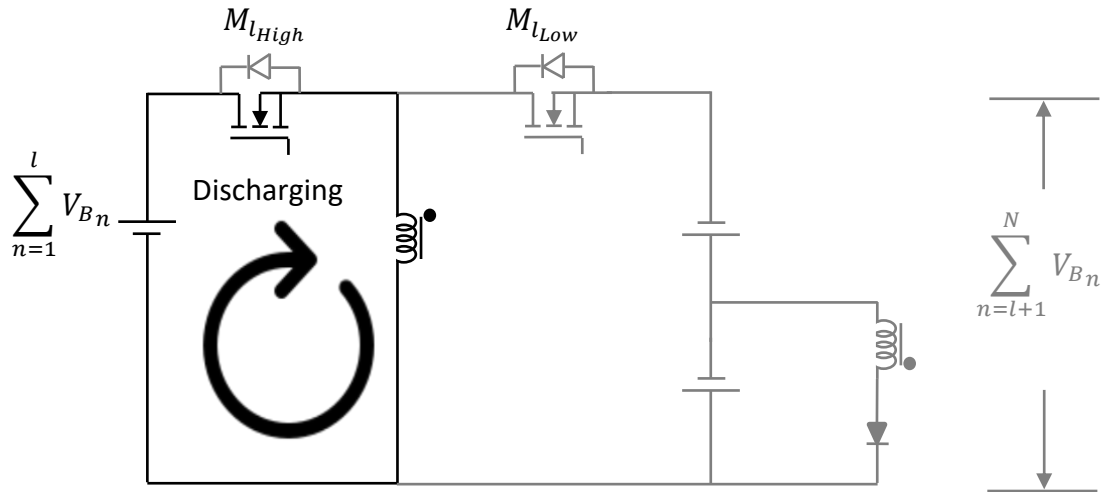


Fig. 3.2 (b) Energy flow for high side MOSFET operation during T_{off}

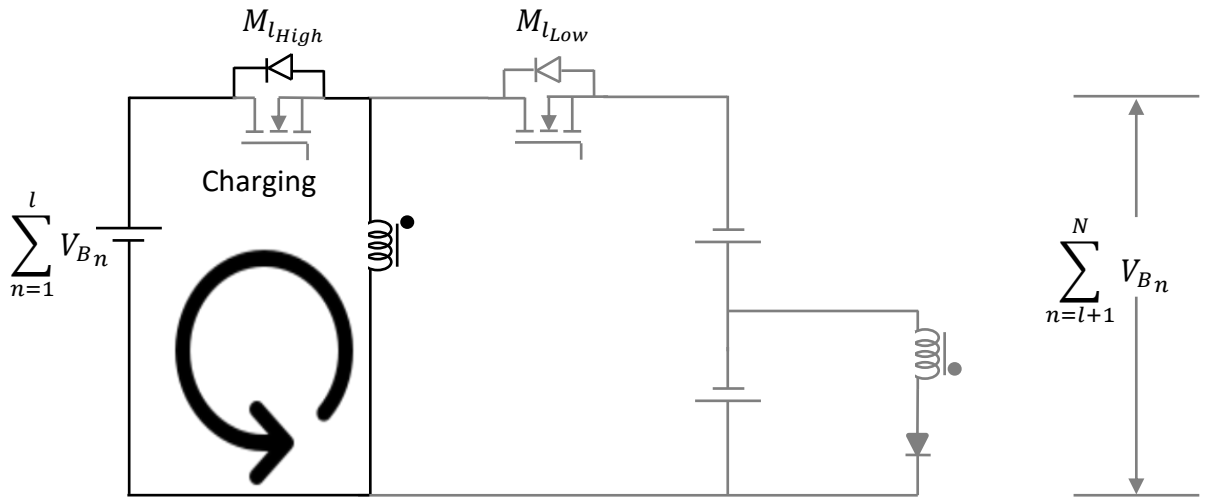


Fig.3.2 (c) Energy flow for low side MOSFET operation during T_{off}

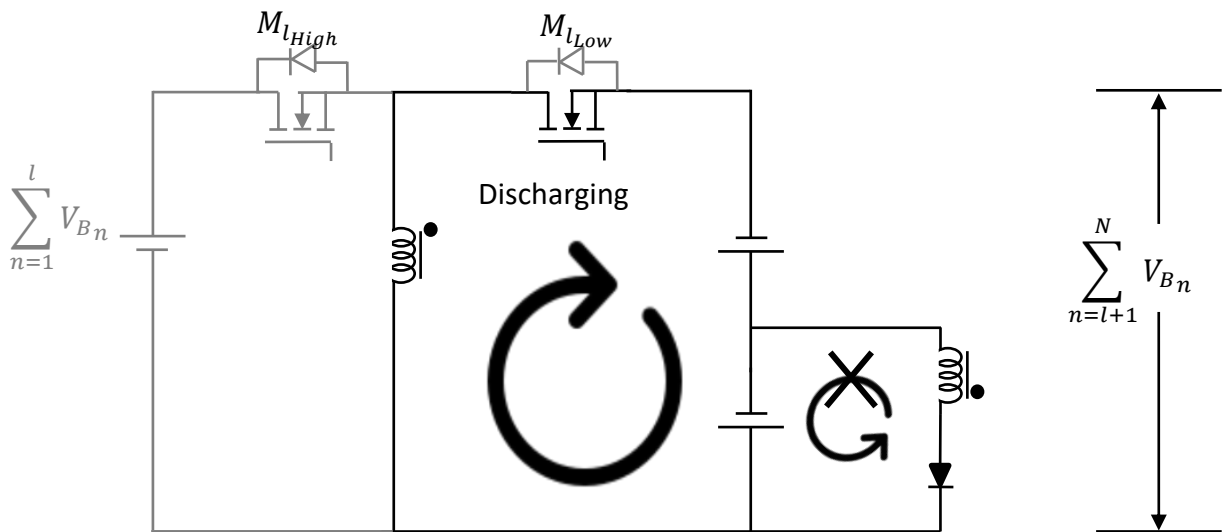


Fig. 3.2 (d) Energy flow for low side MOSFET operation during T_{on}

3.2 MCBB

3.2.1 MCBB Architecture

Similar to MMBE, this architecture of MCBB can be generalized for any number of battery cells in series as shown in Fig. 3.3. For N cells in string, there will be $N - 1$ parallel PEL_t ($t=1,2,3\dots N - 1$). Each PEL ensures bidirectional energy flow and is composed of two MOSFETs (M_{H_t} : high side MOSFETs and M_{L_t} : ground referred low side MOSFETs), coupled inductors (L_{T_t} : inductor at each PEL , L_{C_t} cross inductors between PEL s and L_{B_t} : inductors across battery cells) and diodes (D_{B_t} : diodes across battery cells and D_{C_t} : cross diodes between PEL s) as shown in Fig. 3.3.

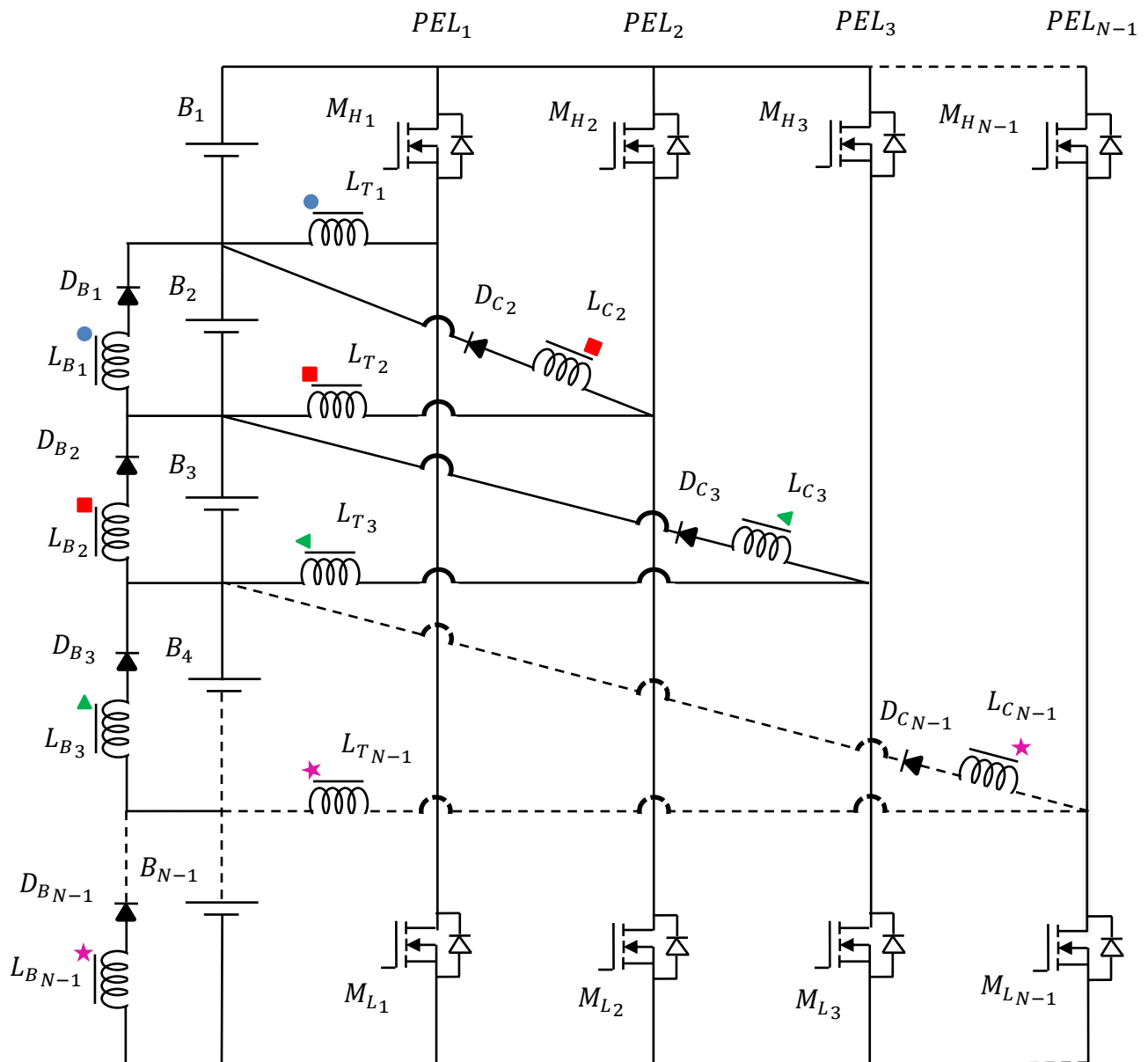


Fig 3.3 Architecture of MCBB equalizer

The cross inductors (L_{C_t}) and diodes (D_{C_t}) in series forms ancillary circuit across PELs (ancillary_cross) and ensure targeted energy transfer for the cell above the operating PEL whereas, inductors (L_{B_t}) and diodes (D_{B_t}) across battery in series forms ancillary circuit across the battery cell (ancillary_battery) and ensures targeted energy transfer for the cell below the operating PEL hence aiding in faster battery balancing. They also act as snubber circuit for the MOSFETs to ease out the voltage stress across it along with stopping the circulating currents due to simultaneous operation of the PELs. PEL 1 doesn't have its corresponding ancillary_cross circuit as they will provide a redundant path from L_{T_1} . Each PEL operates independently to achieve targeted battery balancing. Only one MOSFET in each PEL will operate at a time to avoid short-circuiting of the battery string.

3.2.2 MCBB Operating Modes

Each PEL divides the battery string into parts (high side and low side battery string- ground referred) divided at point of coupling of after L_{T_t} . Average voltage of both the battery string sides (A_{H_t} :average voltage of high side string and A_{L_t} :average voltage for low side battery string) are computed and compared based on which each PEL can have two modes of operation and each mode has two operating states: charging and discharging. Fig. 3.4 shows the operation of PEL 2 for both the modes.

$$\text{String voltage} = \sum_{n=1}^N V_{B_n}; \quad (3.1)$$

$$A_{H_t} = \frac{\sum_{n=1}^t V_{B_n}}{t}; \quad (3.2)$$

$$A_{L_t} = \frac{\sum_{n=t+1}^N V_{B_n}}{N-t} \quad [\cdot V_{B_n} = \text{voltage of battery } n; (n=1,2,\dots,N)] \quad (3.3)$$

Operating mode I: $A_{H_t} > A_{L_t}$

In this mode, M_{H_t} is operated by PWM signals from the control logic and M_{L_t} is kept off.

Charge state: M_{H_t} is switched ON and M_{L_t} is kept OFF. High side battery string discharges itself and stores its energy in L_{T_t} . The current direction is shown in Fig. 3.4(a). L_{T_t} is charged at this time.

Discharge state: M_{H_t} is switched OFF and M_{L_t} is still kept OFF. The energy stored in L_{T_t} in charge state is released to low side battery string and the circuit is completed through the M_{L_t} body diode. The direction of the current is shown in Fig. 3.4 (b). The ancillary_battery circuit also transfers the energy targeting to the successive battery cell B_{t+1} through inductors L_{B_t} . Diode D_{B_t} is forward biased and ensures energy transfer only in one direction and blocks the reverse current. The ancillary_cross circuit is disabled as diode D_{C_t} blocks the reverse current through it.

Operating mode II: $A_{H_t} < A_{L_t}$

In this mode, M_{L_t} is operated by PWM signals from the control logic and M_{H_t} is kept off.

Charge state: M_{L_t} is switched ON and M_{H_t} is kept OFF. Low side battery string discharges itself and stores its energy in L_{T_t} . The current direction is shown in Fig. 3.4(c). L_{T_t} is charged at this time.

Discharge state: M_{L_t} is switched OFF and M_{H_t} is still kept OFF. The energy stored in L_{T_t} in charge state is released to high side battery string and the circuit is completed through the M_{H_t} body diode. The direction of the current is shown in Fig. 3.4 (d). The ancillary_cross circuit also transfers the energy targeting to the battery cell B_t through inductors L_{C_t} . Diode D_{C_t} is forward biased and ensures energy transfer only in one direction and blocks the reverse current. The ancillary_battery circuit is disabled as diode D_{B_t} blocks the reverse current through it.

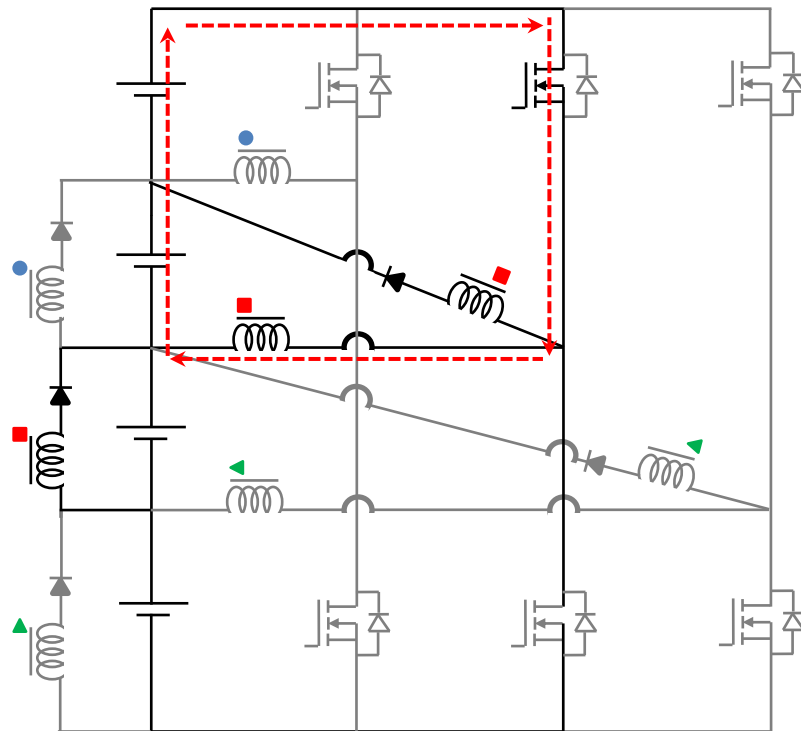


Fig. 3.4 (a) Charging state of operating mode I

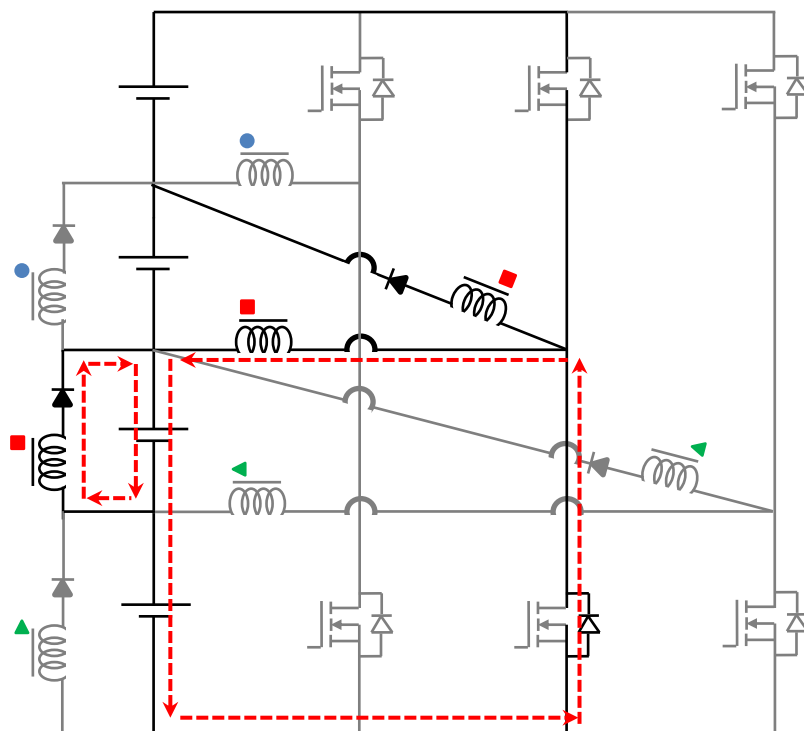


Fig. 3.4 (b) Discharging state of operating mode I

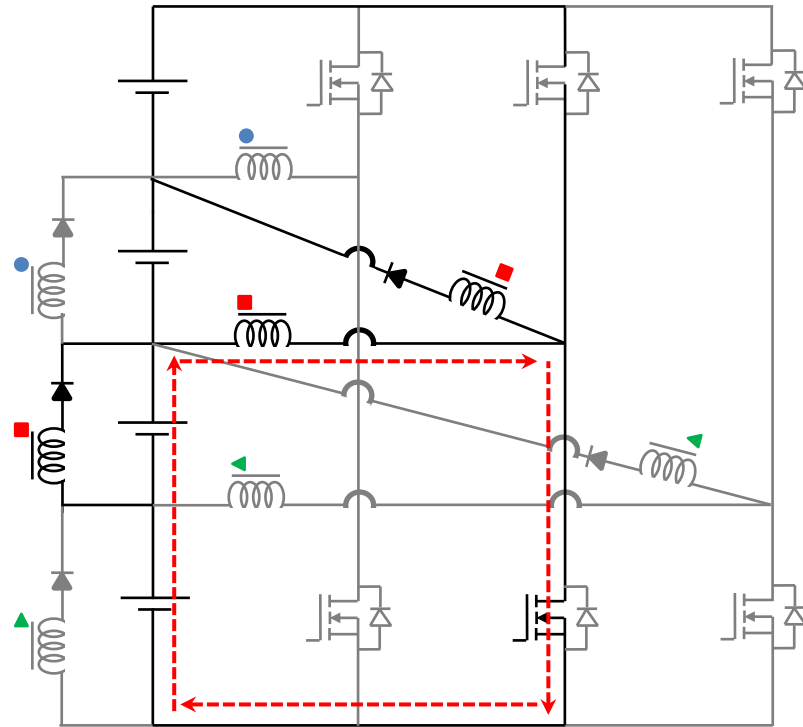


Fig. 3.4 (c) Charging state of operating mode II

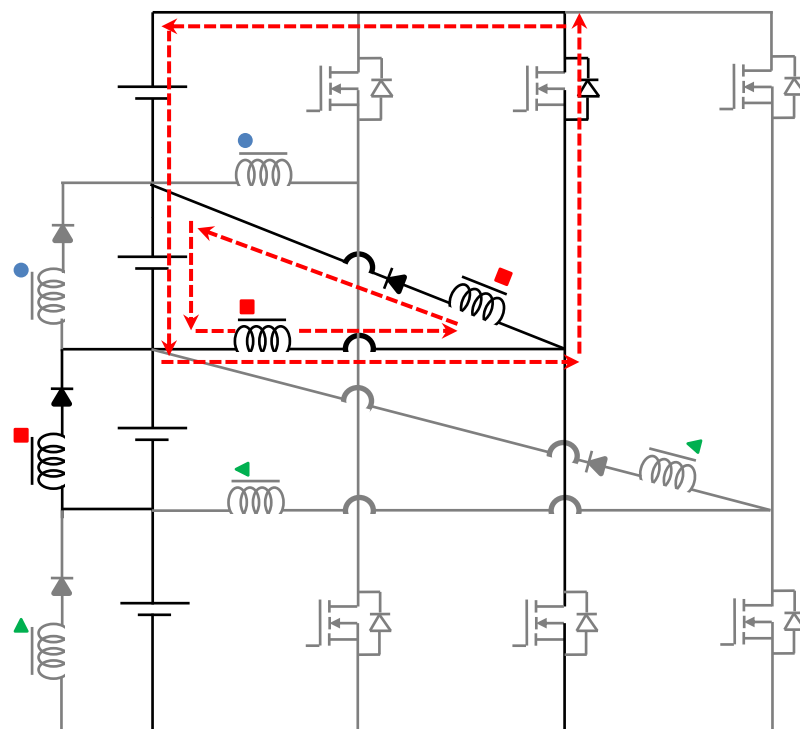


Fig. 3.4 (d) Discharging state of operating mode II

It is to be noted that each PEL can operate in buck or boost mode for energy flow based on the number of battery cells in input side and output side, with respect to the operating MOSFET in that PEL. Like, in case of four battery cells in a string, PEL 1 will operate in boost mode when M_{H_1} is operating whereas, PEL 1 will operate in buck mode when M_{L_1} is operating. Similarly, PEL 3 will operate in buck mode when M_{H_3} is operating and boost mode when M_{L_3} is operating.

The subsequent chapters deal with the generation of pulses to the selected MOSFETs.

CHAPTER 4

SWITCHING ALGORITHM

4.1 Motive of Switching Algorithm

The switching algorithm decides which among the two MOSFETs in a PEL needs to be operated based on the voltages of the battery in the string. As each PEL transfers energy from one half of the string to other, we want that MOSFET to be operated that could transfer energy from higher energy part of the string to lower energy part of the string. This decision is taken by switching algorithm. It actually enables or disables the MOSFET controllers, which is dealt with in next chapter.

The switching algorithm follows a simple decision flow chart to decide which among the two MOSFETs in a PEL is enabled and the other is disabled.

4.2 Switching Algorithm logic and flow chart

The switching algorithm decides which among the two MOSFETs in a PEL needs to be operated. Firstly, battery voltages V_{B_n} ($n=1,2,\dots,N$) are sensed through 'N' voltage dividers coupled to each point of coupling of PEL, referred to ground. The string is divided into two parts for each PEL at the point of common coupling of the string and PEL: high side and low side. The operation of MOSFET is decided by comparing the average voltages of sub-parts of the string under the preview of the PEL, one part above the point of coupling of PEL to the string ($Av_{l_{High}}$) and the other part below the point of coupling of PEL to the string ($Av_{l_{Low}}$).

The algorithm aims to equalize the battery cells for a difference (Diff) of more than 10mV. So "Diff" is calculated by finding difference between maximum voltage of the cell among the string and the lowest voltage of the cells among the string. The average

voltages are calculated for both the sub parts (high side and low side parts) $Av_{l_{High}}$ and $Av_{l_{Low}}$ and then compared. According to this, the decision is taken to enable high side MOSFET ($E_{l_{High}}$) or low side MOSFET ($E_{l_{Low}}$). The equations for switching algorithm is presented below along with decision flow chart in Fig. 4.1.

$$\text{Total String voltage} = \sum_{n=1}^N V_{B_n}; \quad (4.1)$$

$$\text{Diff} = \max(V_{B_1}, V_{B_2} \dots V_{B_{N-1}}) - \min(V_{B_1}, V_{B_2} \dots V_{B_{N-1}}) \quad (4.2)$$

$$\text{Average high side voltage: } Av_{l_{High}} = \frac{\sum_{n=1}^l V_{B_n}}{l}; \quad (4.3)$$

$$\text{Average low side voltage: } Av_{l_{Low}} = \frac{\sum_{n=l+1}^N V_{B_n}}{N-l}; \quad (4.4)$$

$$\text{Enable for high side MOSFET: } E_{l_{High}} = \begin{cases} 1 : Av_{l_{High}} > Av_{l_{Low}} \\ 0 : Av_{l_{High}} \leq Av_{l_{Low}} \end{cases} \quad (4.5)$$

$$\text{Enable for low side MOSFET: } E_{l_{Low}} = \begin{cases} 1 : Av_{l_{Low}} > Av_{l_{High}} \\ 0 : Av_{l_{Low}} \leq Av_{l_{High}} \end{cases} \quad (4.6)$$

The values of $Av_{l_{High}}$ and $Av_{l_{Low}}$ are calculated and based on which among them is greater, decision is taken for enabling signals $E_{l_{High}}$ and $E_{l_{Low}}$. These enabling signals decides on which MOSFET among the two in each PEL will operate and the enable signal is combined with the PWM signal for the MOSFETs that is obtained by the control logic dealt in the succeeding section

The voltage controller thus can operate in buck or boost mode based on switch operation in a PEL for energy flow from higher side of battery cells to lower side referred to point of coupling in the sub-string or vice-versa.

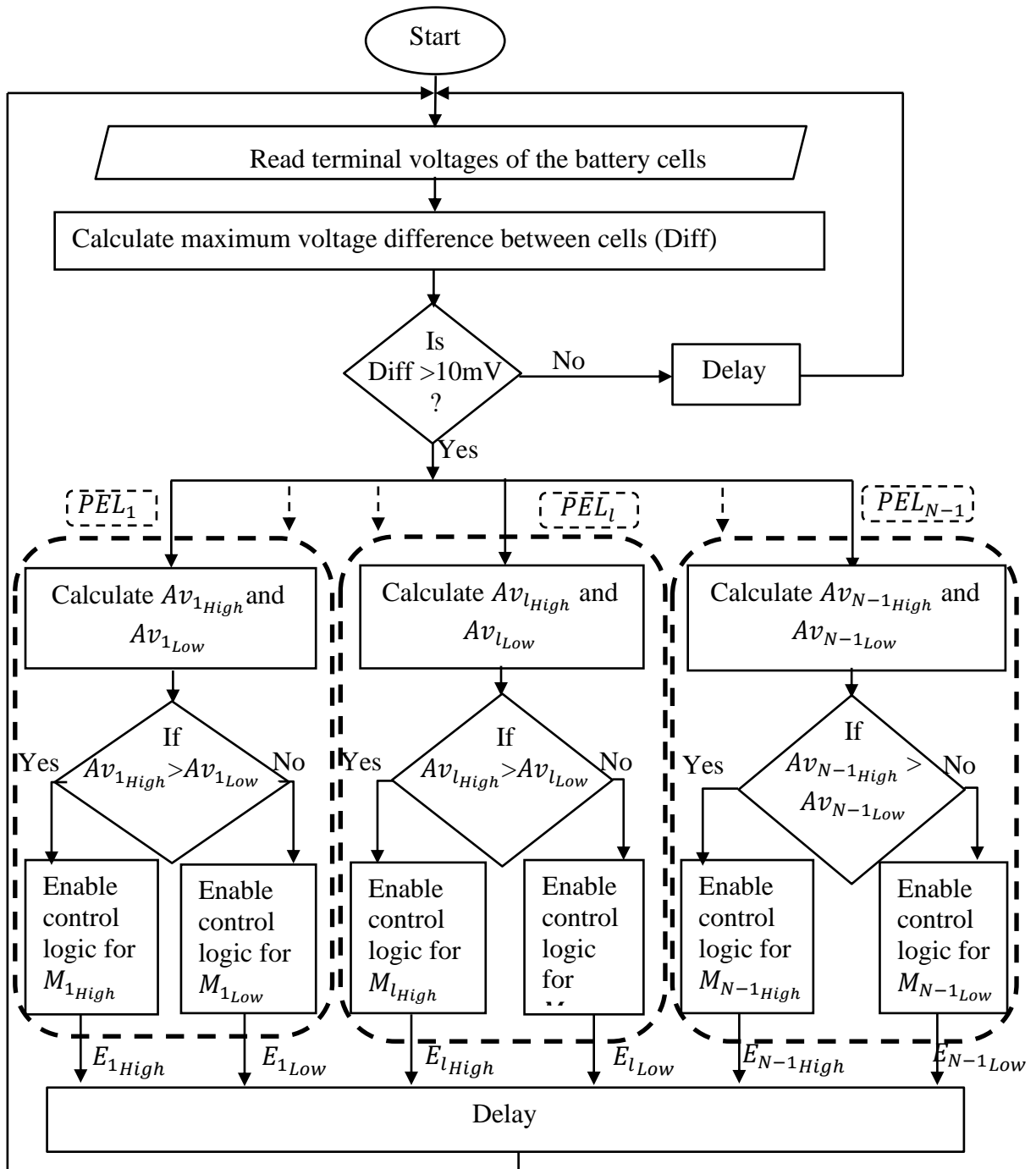


Fig. 4.1 Switching Algorithm for enabling controller MOSFETs from controller

CHAPTER 5

CONTROL STRATEGY

5.1 Motive of Control Strategy

Dual loop control strategy is used to operate the MOSFETs in both MMBE and MCBB. The outer loop is voltage controlled and inner loop is current controlled. This helps in achieving the controlling of inductor current for each PEL. The design can be customised according to the requirement and thus value of balancing current can be chooses based of how fast or slow balancing needs to be achieved. Cascaded PI controllers are used for simple control of voltages and current. It is combined with switching algorithm, dealt with in previous chapter, to enable or disable the particular MOSFET.

5.2 Dual Loop Current Control

The suitable control logic for MMBE is the one that is based on dual loop control scheme as shown in Fig. 4. The inner loop is a current controlled loop and outer loop is a voltage controlled loop. The switching algorithm presented in previous section enables the “on” or “off” state of the switches and in turn support the control logic for PWM generation and control of MMBE.

To ensure convergence of batteries on both sides of PEL at the point of coupling, the error between $Av_{l_{High}}$ and $Av_{l_{Low}}$ for each PEL is fed to PI voltage controller. A constant feedforward reference is added/ subtracted as per high/low side switch operation, to devise the reference current for current control $i_{L_l}^*$. For high side current reference,

$$i_{L_{1H}}^* = K_{P_{v_H}}(Av_{l_{High}} - Av_{l_{Low}}) + K_{I_{v_H}} \int (Av_{l_{High}} - Av_{l_{Low}}) dt + C \quad (5.1)$$

For low side current reference,

$$i_{L_{1L}}^* = K_{P_{v_L}}(Av_{l_{Low}} - Av_{l_{High}}) + K_{I_{v_L}} \int (Av_{l_{Low}} - Av_{l_{High}}) dt + C \quad (5.2)$$

The $K_{P_{v_H}}$ and $K_{I_{v_H}}$ are proportional and integral gain value for high side voltage controller, and similarly $K_{P_{v_L}}$ and $K_{I_{v_L}}$ are the are proportional and integral gain value for low side voltage controller respectively. The constant value “C” is the current reference value in “Amperes” for which the balancing needs to be done according to the design.

This current reference is now compared with actual current value across the PEL inductor L_{P_l} and its error is fed to PI current controller. The output of current controller forms the modulating signal (d'_l) for PWM block to devise the switching signals for corresponding MOSFETs selected by enable logic presented in preceding subsection.

$$d'_{1H} = K_{P_{i_H}}(i_{L_{1H}}^* - i_{L_1}) + K_{I_{i_H}} \int (i_{L_{1H}}^* - i_{L_1}) dt \quad (5.3)$$

$$d'_{1L} = K_{P_{i_L}}(i_{L_{1L}}^* - i_{L_1}) + K_{I_{i_L}} \int (i_{L_{1L}}^* - i_{L_1}) dt \quad (5.4)$$

The $K_{P_{i_H}}$ and $K_{I_{i_H}}$ are proportional and integral gain value for high side current controller, and similarly $K_{P_{i_L}}$ and $K_{I_{i_L}}$ are the are proportional and integral gain value for low side current controller respectively.

The pulses are generated such that it controls the voltages of the batteries and switches them to converge at the average point along with maintaing the balancing current at the value of “C” given according to the design.

The pulses are combined with switching algorithm in the end with an AND logic gate which acts as enable signal.

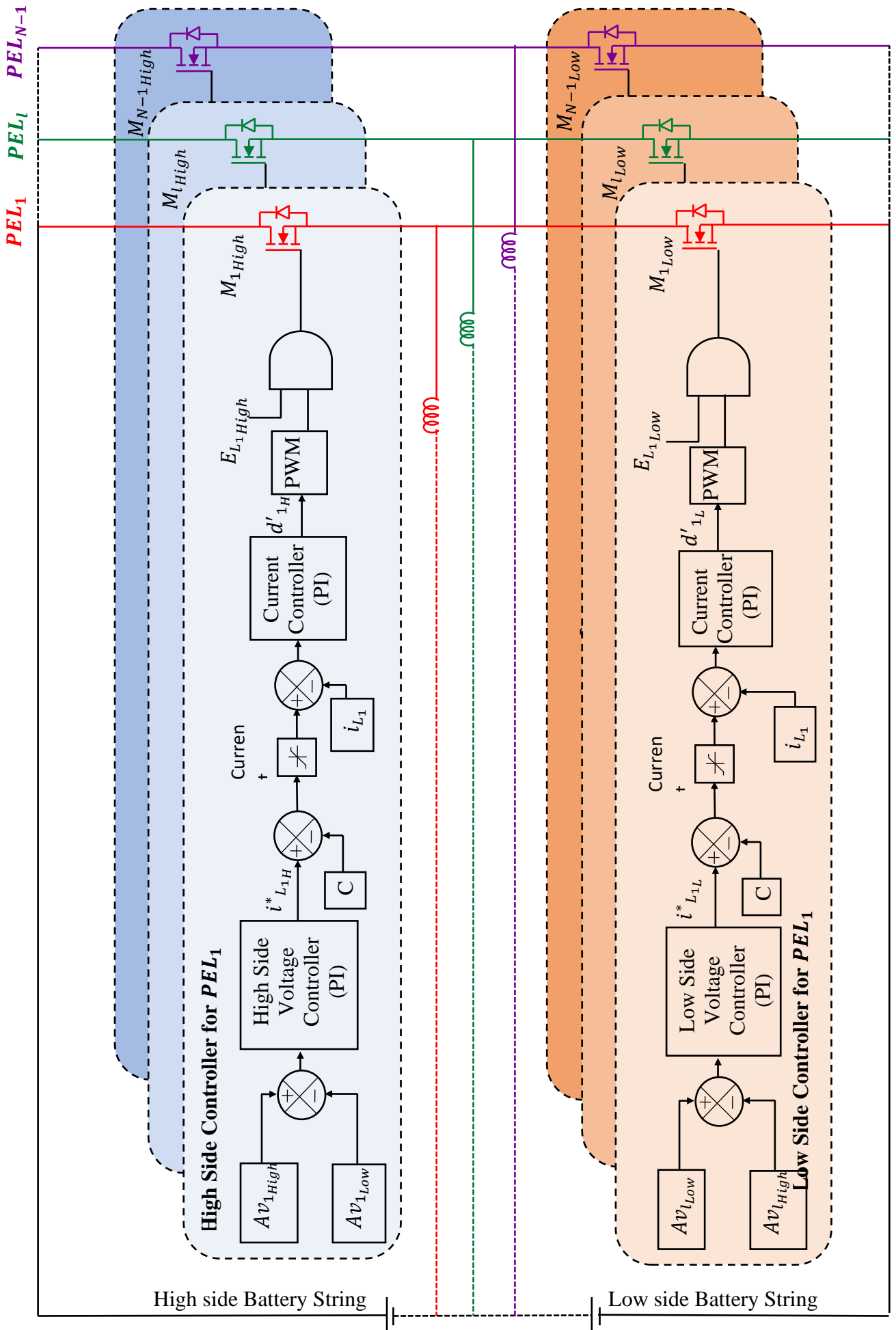


Fig. 5.1 Control strategy for MMBE and MCBB equalizers

CHAPTER 6

PERFORMANCE ANALYSIS

6.1 System Configuration

Energy storage systems are quite expensive and so, good management and operation is required to ensure optimum consumption, increased performance, and longer lives. Frequent maintenance, deterioration, early failure, and poor performance are all issues that arise as a result of inappropriate voltage distribution in the cells connected in series forming a string. As a result, it is clear that cell balancing methods have a significant impact on storage system performance. A well-planned voltage equalizer for transferring charge within the cells in the string is currently regarded as an important field of research and development.

Both the proposed equalizers MMBE and MCBB are modelled in MATLAB/Simulink. The switching algorithm is coded in MATLAB function block and its enable output is combined with the control strategy using an AND logic operator as described in earlier chapters. This chapter describes the simulation and execution of two proposed voltage equalisation algorithms, as well as an analysis of their effects on the overall performance of the storage system.

The prime purpose of the Battery Balancing system is to monitor and balance the cells in the string that forms the storage system. The storage system considered is a lead acid battery system implemented to absorb or supplement the generated power. Four lead acid batteries are taken in a string to form a 48V battery storage system. Number of batteries in parallel is decided on the capacity required for the storage system. Each lead acid battery has specifications of 40Ah capacity and nominal voltage of 12V.

For evaluating the performance of MMBE and MCBB, four batteries are taken in series with different State of Charge (SOC) levels. Both the equalizers have same specifications, enlisted in Table 6.1. The switching frequency for converters is chosen as 100kHz. The coupled inductors have parameters $L_{p_l}=L_{D_l}=150\ \mu\text{H}$ with coefficient of coupling 90%. All the MOSFETS have $R_{DSon}=0.01\ \Omega$. The reference current value for feedforward current “C” is taken as 5A.

TABLE 6.1. CONVERTER AND BATTERY CELL DATA

Parameters	Value
Number of Batteries in string	4
Nominal voltage of battery	12 V
Rated Capacity of battery	40 Ah
L_{p_l} (l=1,2,3)	150 μH
L_{D_l} (l=1,2,3)	150 μH
Switching Frequency	100 kHz
R_{DSon} of MOSFETs	0.01 Ω
Feedforward constant “C”	5
Forward voltage drop across diode D_l	0.8 V

As SOC level is the measure of stored capacity in the battery and is directly related to the voltage of the battery, we change SOC values and check the effectiveness of the equalizer.

For four batteries in the string following 14 cases can be created based on the SOC levels of the batteries and their positions in the string, when compared to the average value of the SOC levels.

Considering average value of SOC level as a zero potential point “0”, any SOC value above the average value is denoted positive “+” and any SOC value below the average SOC level is denoted negative “-”. Any string will have atleast one “-” or one “+” denoted battery cell, because average value of SOC levels is the sum of all the SOC values of the batteries divided by the number of batteries. thus only 14 cases are possible.

B_n = SOC level of battery positioned at “n” places from top. (n = 1,2,3,4)

B_{Avg} = Average of SOC levels of the batteries in the string.

$$B_{Avg} = \frac{\sum_{n=1}^4 B_n}{4} \quad (6.1)$$

S_{Vn} = Sign denotation given to each battery when compared to its average SOC level.

$$S_{Vn} = \begin{cases} + : B_n > B_{Avg} \\ 0 : B_n = B_{Avg} \\ - : B_n < B_{Avg} \end{cases} \quad (6.2)$$

Now sign denotation is given for each PEL part of battery string (high side part and low side part) based on the average SOC of that part is less than or greater than B_{Avg} .

$$\text{Average SOC level of high side for PEL}_n: ASOC_{l_{High}} = \frac{\sum_{n=1}^l B_n}{l} \quad (6.3)$$

$$\text{Average SOC level of low side for PEL}_n: ASOC_{l_{Low}} = \frac{\sum_{n=l+1}^4 B_n}{4-l} \quad (6.4)$$

$S_{n_{High}}$ = Sign denotation for high side Mosfet in PEL_n

$$S_{n_{High}} = \begin{cases} + : ASOC_{l_{High}} > B_{Avg} \\ 0 : ASOC_{l_{High}} = B_{Avg} \\ - : ASOC_{l_{High}} < B_{Avg} \end{cases} \quad (6.5)$$

$S_{n_{Low}}$ = Sign denotation for low side Mosfet in PEL_n

$$S_{n_{Low}} = \begin{cases} + : ASOC_{l_{Low}} > B_{Avg} \\ 0 : ASOC_{l_{Low}} = B_{Avg} \\ - : ASOC_{l_{Low}} < B_{Avg} \end{cases} \quad (6.5)$$

For all 14 types of cases, some arbitrary value of SOC levels are taken for the battery string and shown in Table 6.2.

TABLE 6.2. POSSIBLE CASES BASED ON DIFFERENT SOC LEVELS OF BATTERY AND ITS POSITION IN STRING

Sr. No	B ₁	B ₂	B ₃	B ₄	B _{Avg}	S _{V1}	S _{V2}	S _{V3}	S _{V4}	PEL 1		PEL 2		PEL 3	
										S _{1High}	S _{1Low}	S _{2High}	S _{2Low}	S _{3High}	S _{3Low}
1	90	80	78	40	72	+	+	+	-	+	-	+	-	+	-
2	88	75	20	98	70.25	+	+	-	+	+	-	+	-	-	+
3	94	24	78	82	69.5	+	-	+	+	+	-	-	+	-	+
4	35	79	84	94	73	-	+	+	+	-	+	-	+	-	+
5	97	84	35	46	65.5	+	+	-	-	+	-	+	-	+	-
6	96	41	83	26	61.5	+	-	+	-	+	-	+	-	+	-
7	36	87	71	26	55	-	+	+	-	-	+	-	-	+	-
8	42	86	39	76	60.75	-	+	-	+	-	+	+	-	-	+
9	48	39	86	81	63.5	-	-	+	+	-	+	-	+	-	+
10	94	38	49	83	66	+	-	-	+	+	-	0	0	-	+
11	23	34	45	82	46	-	-	-	+	-	+	-	+	-	+
12	23	34	82	45	46	-	-	+	-	-	+	-	+	+	-
13	23	82	45	34	46	-	+	-	-	-	+	+	-	+	-
14	82	34	45	23	46	+	-	-	-	+	-	+	-	+	-

It is very easy to understand based on the above table, which subpart has higher SOC value weightage than the average in a given PEL. Thus we can decide the direction of energy transfer. Hence, which MOSFET needs to be operated is also decided based on this. In each PEL, the

Both the equalizers MMBE and MCBB behaved as expected for all the above test cases. They try to equalize the capacity in the string and bring it to average value. Each PEL operates in such a way that it transfers energy from higher capacity subpart to lower capacity subpart of the string. The PEL operation stops if the average of the high side and low side subpart is equal to the average of the entire string.

Two separate cases are considered to show the effectiveness of the equalizers in the subsequent sub-sections using MMBE and MCBB equalizers respectively.

6.2 Cases Considered for Effectiveness of Equalizer MMBE

Amongst fourteen cases, two distinct cases of different SOC levels of batteries in string are considered to demonstrate the effectiveness of proposed MMBE and its control as in Table 6.3. Since the difference of SOC of batteries directly relates to the difference in voltage, the voltages across batteries are sensed to run the proposed algorithm, described in chapter 4.

Case I marks the descending SOC levels, batteries with highest SOC at the top and lowest SOC at bottom of the string. The average of SOC for all the batteries in the string is 69. As per the proposed algorithm (shown in Fig. 4.1), the average values are computed and switching vectors for the controller to enable the MOSFETs in the corresponding PELs are generated. For the present case M_{1High} , M_{2High} and M_{3High} are switched “on” and M_{1Low} , M_{2Low} and M_{3Low} are switched “off”, allowing their body diodes to participate in the energy transfer. Since all PELs are operating, it will ensure faster equalization. The battery voltage farthest from the average value transfers/ receives highest energy. Whereas, the balancing algorithm in [55] can operate only with one PEL,

TABLE 6.3. DIFFERENT CASES OF BATTERY SOC LEVELS DEMONSTRATING PARALLEL OPERATION OF PEL IN MMBE

	B ₁	B ₂	B ₃	B ₄	B _{Avg}	Average voltages in sub-strings						MMBE switch selection			PEL selection [55]		
						A _{1High}	A _{1Low}	A _{2High}	A _{2Low}	A _{3High}	A _{3Low}	PEL ₁	PEL ₂	PEL ₃	Leg ₁	Leg ₂	Leg ₃
Case I	94	81	54	47	69	94	60.66	87.5	50.5	76.33	47	M_{1High}	M_{2High}	M_{3High}	Disabled	High side MOSFET operates	Disabled
						Diff=33.34		Diff=37		Diff=29.33							
Case II	50	81	90	60	70.25	50	77	65.5	75	73.66	60	M_{1Low}	M_{2Low}	M_{3High}	Low side MOSFET operates	Disabled	Disabled
						Diff=27		Diff=9.5		Diff=13.66							

based on maximum voltage difference. This makes equalization slower as only one leg can be operated, thus the battery voltage farthest from the average voltage will require maximum time to reach the average voltage.

For case II, SOC levels are randomly ordered, where highest SOC level of battery is considered in the middle of the string. Average SOC levels of each group and their differences are calculated as per proposed algorithm and switches in the PELs are operated. Accordingly, M_{1Low} , M_{2Low} and M_{3High} are operated in corresponding PEL of MMBE. Whereas, as per [55] low side MOSFET of Leg1 will operate and tend to diverge the SOC levels and voltage difference away from the average value, and thus shall fail to deliver.

6.2.1 Case I

Fig. 6.1 shows the run time voltage waveform of batteries for case I. For the duties of the switches decided by dual loop controller, the voltage of all the four batteries converges and comes to its average voltage at 2.8msec though charge may not get equalized. The input and the output side batteries clamp each other and depicts run time voltage as average voltage. In fact, the actual open circuit voltage (OCV) depicts the equalization of SOC. Fig. 6.2 depicts the SOC levels of the battery in string and Fig. 6.3 shows inductor currents, while Table 6.4 shows the SOC and voltage relation for case I after 0.5sec. It may be observed that SOC conversion is directed for all batteries, and the battery which is farthest from average SOC experience greater slope than those nearer to the average SOC. Further to establish the charge balancing is continuing with control of MMBE, the process of charging is periodically relinquished and re-established, which is shown in Fig. 6.4 for case I, it may be clearly observed that slowly the OCV voltages also

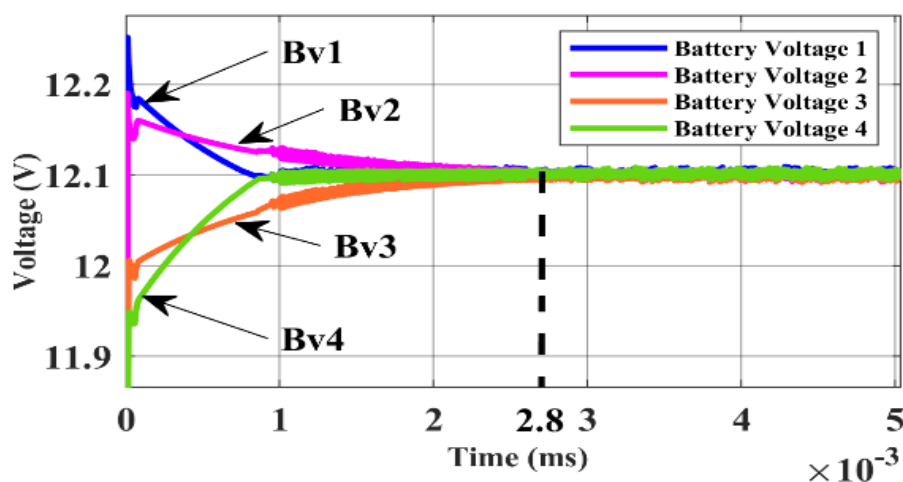


Fig 6.1: Voltage waveform for Case I in MMBE

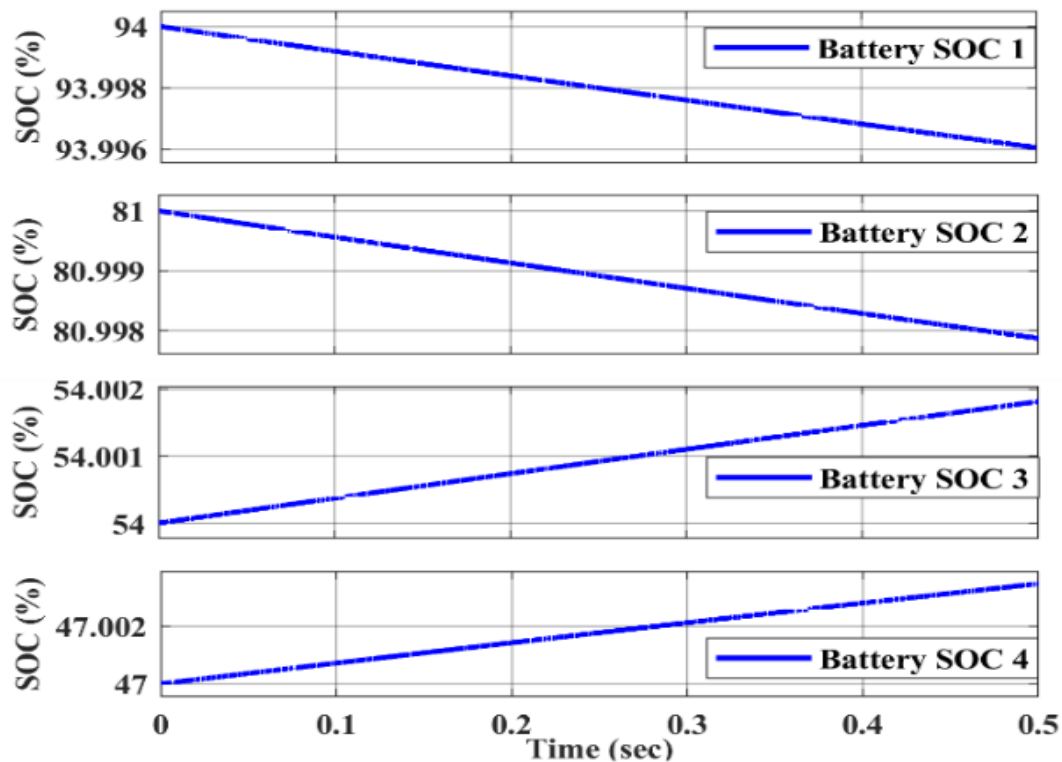


Fig. 6.2 SOC waveform for case I in MMBE

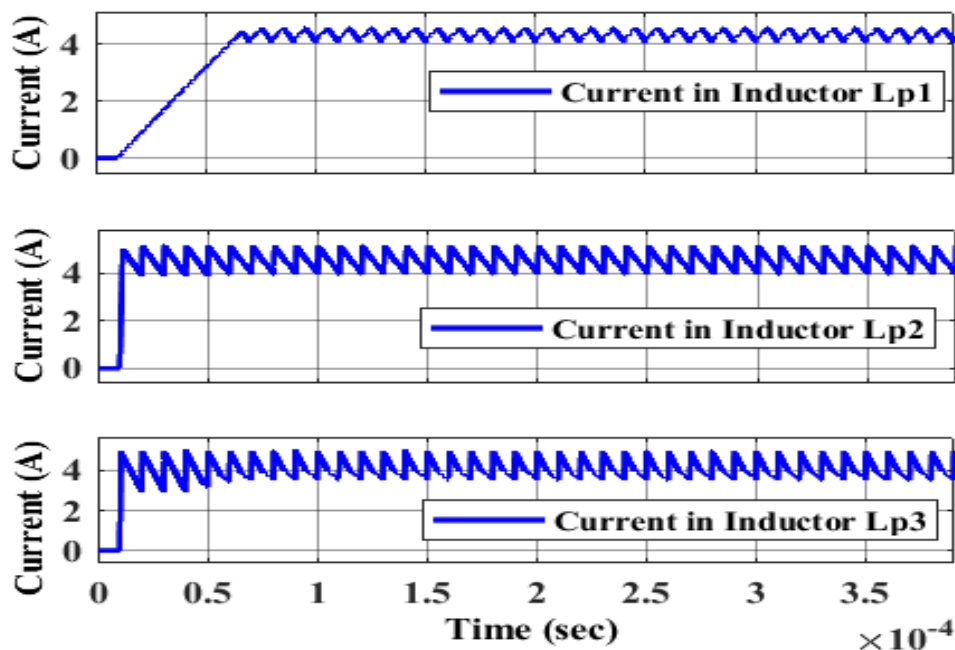


Fig. 6.3 Inductor current waveform for case I in MMBE

start to converge giving confidence of equalization, as simulation cannot be run for longer time due to storage and computation limitations. The SOC levels are depicted for intermittent equalization are shown in Fig. 6.5, which display small ripples reflecting make and break of MMBE based equalization process.

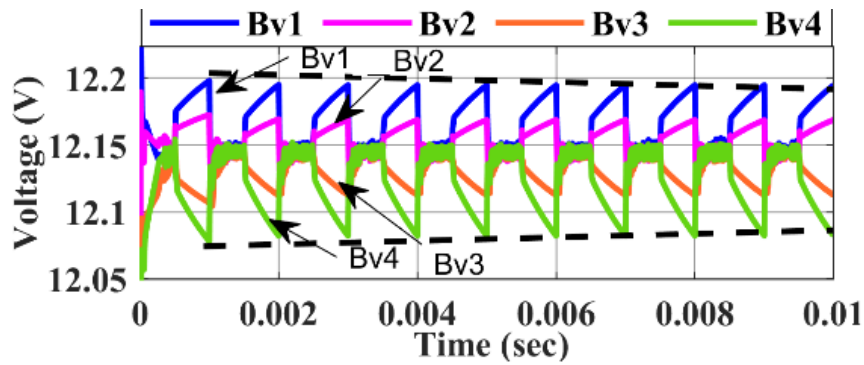


Fig. 6.4 Voltage waveform for case I with delay for ensuring OCV

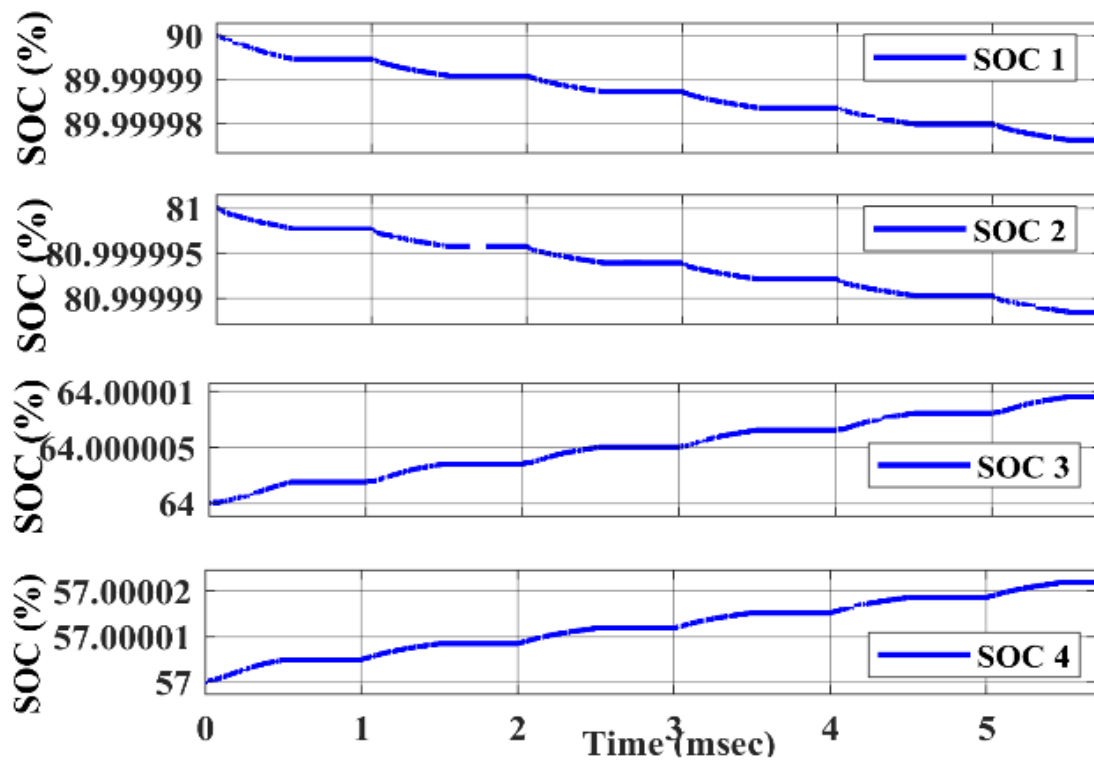


Fig. 6.5 SOC waveform for case I with delay

TABLE 6.4. SOC AND VOLTAGE RELATION FOR CASE I BEFORE STARTING EQUALIZATION AND AFTER 0.5 SEC OF EQUALIZATION

	Voltage before Balancing	Voltage After Balancing	Soc before Balancing	SOC after 0.5 sec
Battery 1	12.22	12.09	94	93.996
Battery 2	12.18	12.09	81	80.9979
Battery 3	12.00	12.09	54	54.0018
Battery 4	11.89	12.09	47	47.0038

6.2.2 Case II

In case II, which depicts the case of jumbled SOC of the batteries in the string for equalization, where the highest voltage battery and the lowest voltage battery are not at the extreme ends. Fig. 6.6 clearly shows that proposed MMBE after targeted equalization and the SOC of the batteries converges towards its average SOC value as per proposed algorithm. Since, M_{1Low} , M_{2Low} and M_{3High} switches operate for case II, hence current in L_{P1} and L_{P2} shall get in reverse direction whereas, current in L_{P3} remains the same (as shown in Fig. 6.7), which could be possible with the flexibility of operation with all the PELs simultaneously, and cannot be achieved by operation of only one leg.

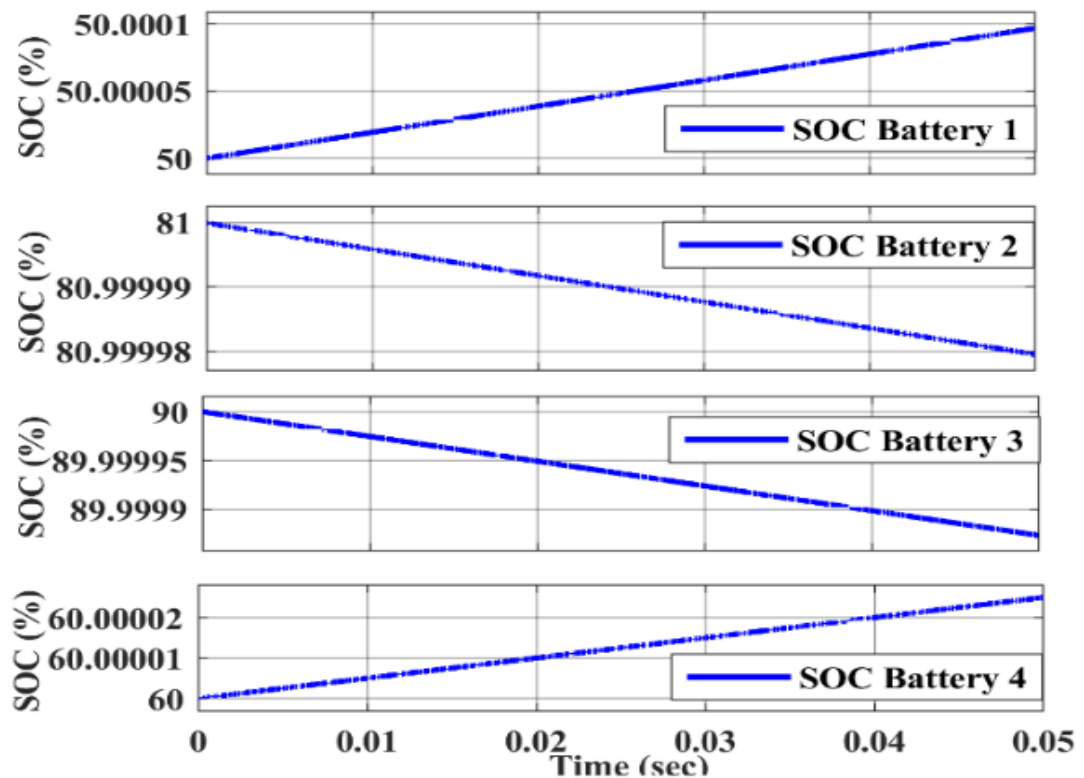


Fig 6.6 SOC waveform for case II in MMBE

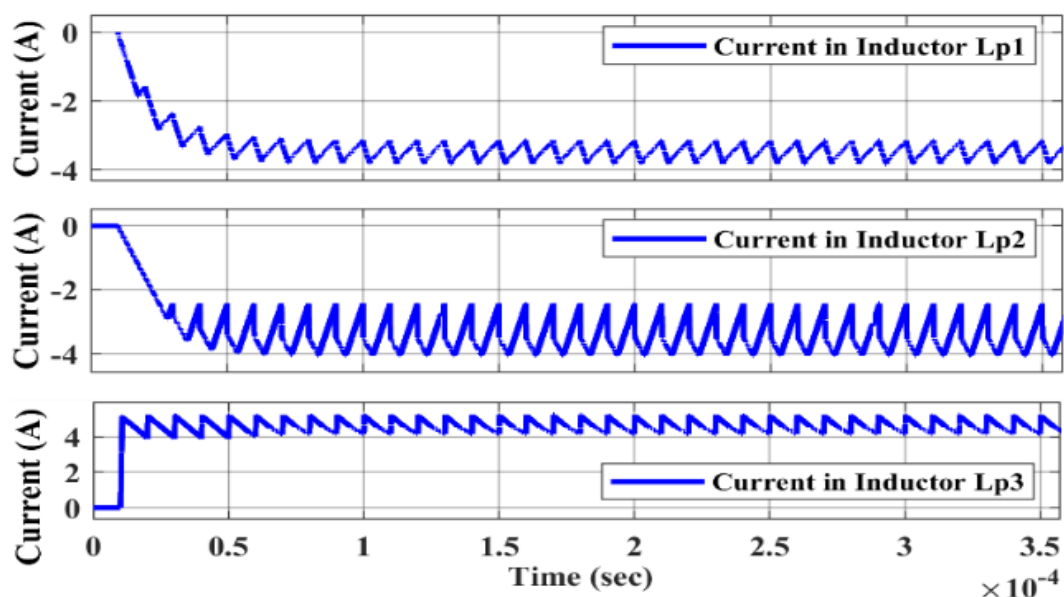


Fig. 6.7 Current waveform for case II in MMBE

The results demonstrate that MMBE is capable of balancing the batteries having random SOC levels with enhanced speed along with targeted balancing with high efficiency operating with parallel paths with low and high side switches.

6.3 Cases Considered for Effectiveness of Equalizer MCBB

Similarly, Two separate cases of varied SOC levels of batteries in string are explored in Table 6.5 to demonstrate the efficacy of the proposed MCBB and its control among fourteen cases. Since the difference in SOC levels of batteries is directly related to the difference in voltage, the voltages across batteries are sensed to execute the suggested algorithm.

TABLE 6.5. DIFFERENT CASES OF BATTERY SOC LEVELS DEMONSTRATING PARALLEL OPERATION OF PEL IN MCBB

	B ₁	B ₂	B ₃	B ₄	B _{Avg}	Average voltages in sub-strings						MCBB switch selection			Leg selection [55]		
						A _{H₁}	A _{L₁}	A _{H₂}	A _{L₂}	A _{H₃}	A _{L₃}	Leg ₁	Leg ₂	Leg ₃	Leg ₁	Leg ₂	Leg ₃
Case I	90	74	58	48	67.5	90	60	82	53	74	48	M _{H1}	M _{H2}	M _{H3}	High side MOSFET operates	Disabled	Disabled
						Diff=60		Diff=37		Diff=29.33							
Case II	58	74	90	65	71.75	58	76.33	66	77.5	74	65	M _{L1}	M _{L2}	M _{H3}	Low side MOSFET operates	Disabled	Disabled
						Diff=18.33		Diff=11.5		Diff=9							

6.3.1 Case I

Case I denotes descending SOC levels, with the highest SOC at the top of the string and the lowest SOC at the bottom. The average of SOC levels of all the four batteries is 67.5 and the average SOC levels for upper part and lower part of each leg and its difference is calculated in Table 1. Based on these values, the switching vectors for the controller to enable MOSFETs in respective Legs is generated using the suggested technique as shown in Table 1. Thus for case I, M_{H1} , M_{H2} , and M_{H3} are operated whereas M_{L1} , M_{L2} , and M_{L3} are kept switched off, allowing their body diodes to participate in the energy transfer. Because all PELs are operational, faster equalization will be possible. The voltage of the battery that is farthest from the average value transfers/receives the most energy. The balancing method in [55], on the other hand, can only work with one leg and the selection of the leg is dependent on the maximum voltage difference. Due to the fact that only one leg can be moved, equalization is slower, and the battery voltage farthest from the average voltage will take the longest time to approach the equalization voltage. Thus with [55] controller high side MOSFET for leg 1 operates for equalization. MATLAB Simulation for MCBB equalizer is performed. Fig. 6.8 depicts the run time voltage waveform of the batteries for case I. It can be seen that the voltage of all four batteries converges and arrives to its average voltage at 0.4msec, albeit charge may not be equalized. The input and output side batteries are clamped together, and the run time voltage is seen as average voltage. In reality, the actual open circuit voltage (OCV) shows how SOC levels are balanced. The SOC levels of the battery in string are depicted in Fig.6.10, and inductor currents are depicted in Fig.6.9. SOC conversion is targeted for all batteries, and the battery that is farthest from average SOC has a steeper slope than those that are closer to the average SOC. Further, to ensure that charge balancing is maintained under MCBB control, the charging process is periodically relinquished and re-established, as shown in Fig. 6.11 for Case I. It can be seen that the OCV voltages gradually begin to converge, indicating equalization, as the simulation cannot be run for longer time due to storage and computation limitations. In Fig. 6.12, the SOC levels for intermittent equalization are presented, with minor ripples reflecting the make and break of the MCBB-based equalization process.

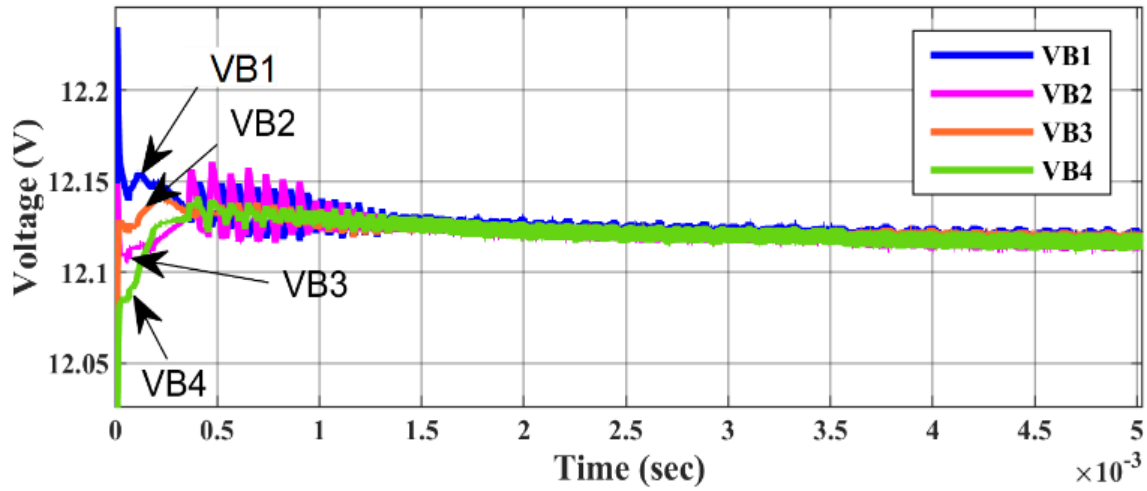


Fig. 6.8 Real time voltage waveform for case I

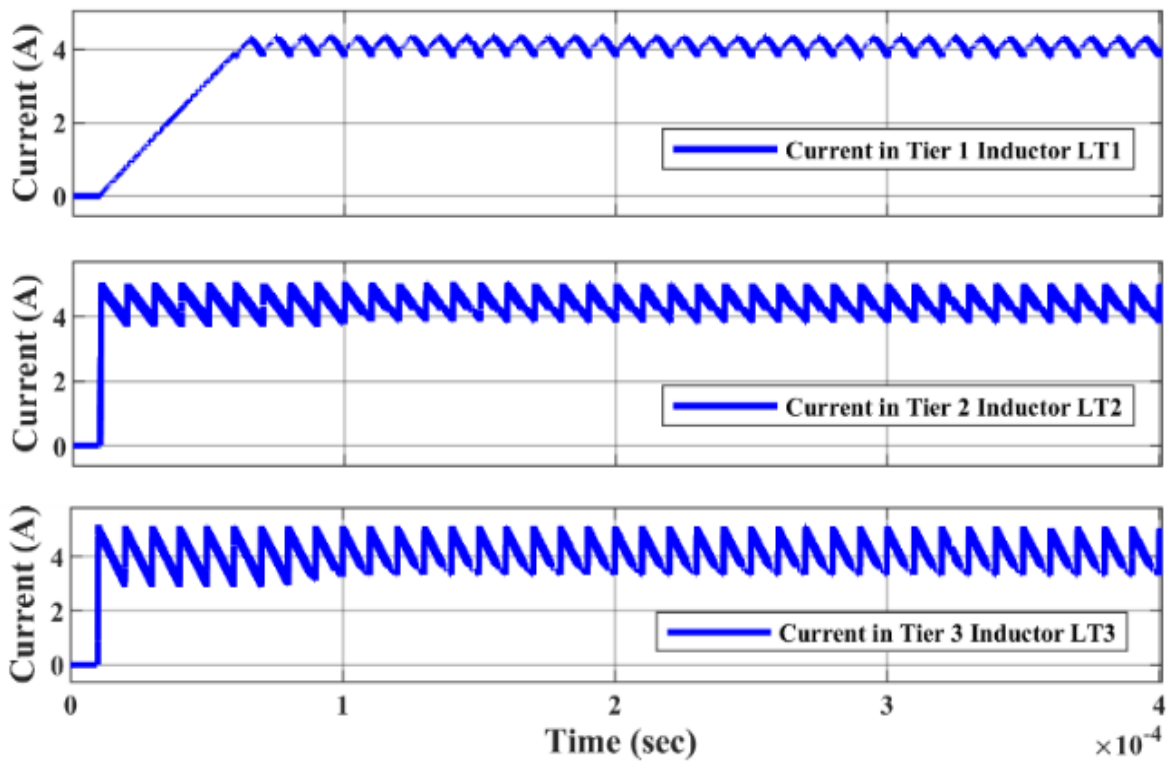


Fig. 6.9: Inductor current waveform for case I

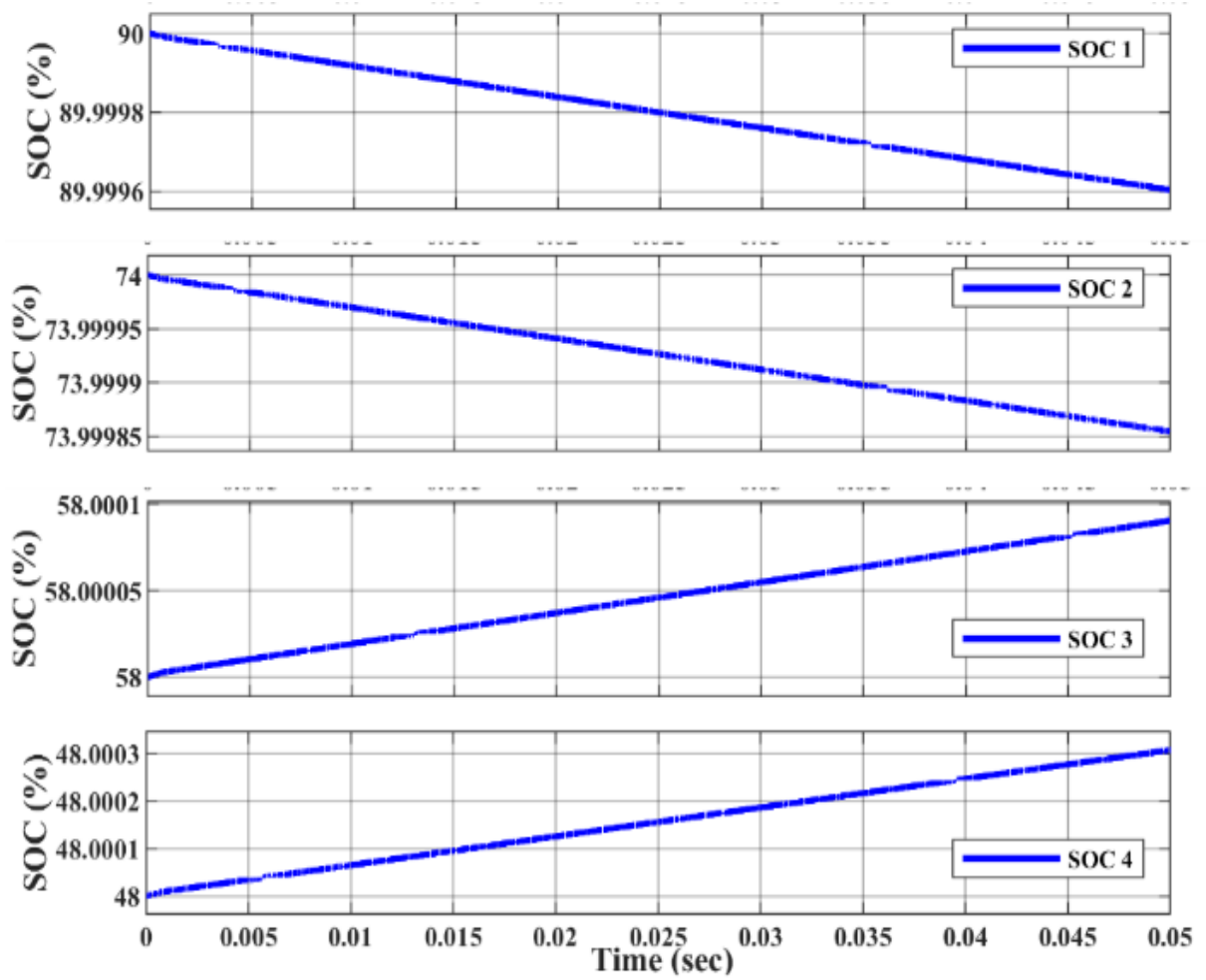


Fig. 6.10 SOC waveform for case I

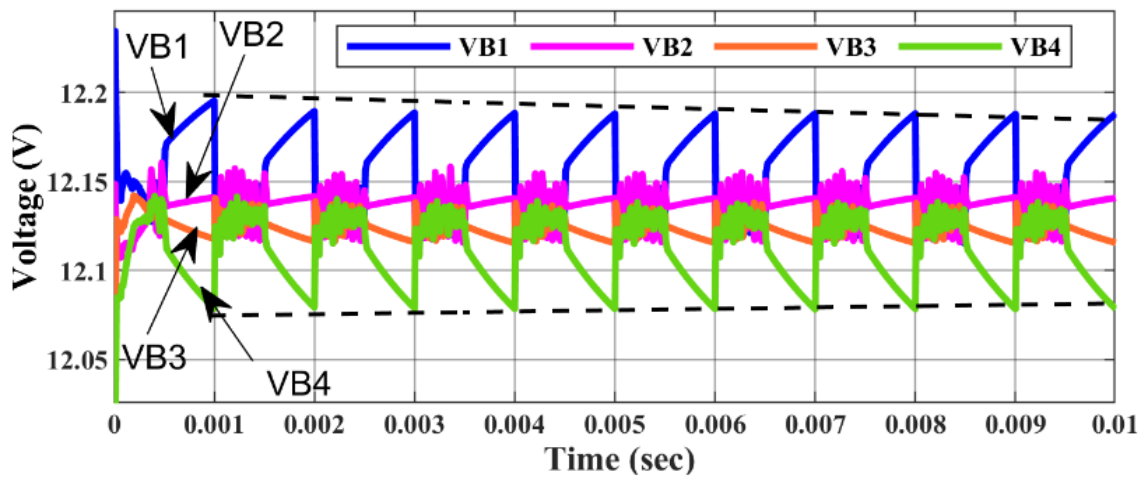


Fig. 6.11 Voltage waveform for case II with delay for ensuring OCV

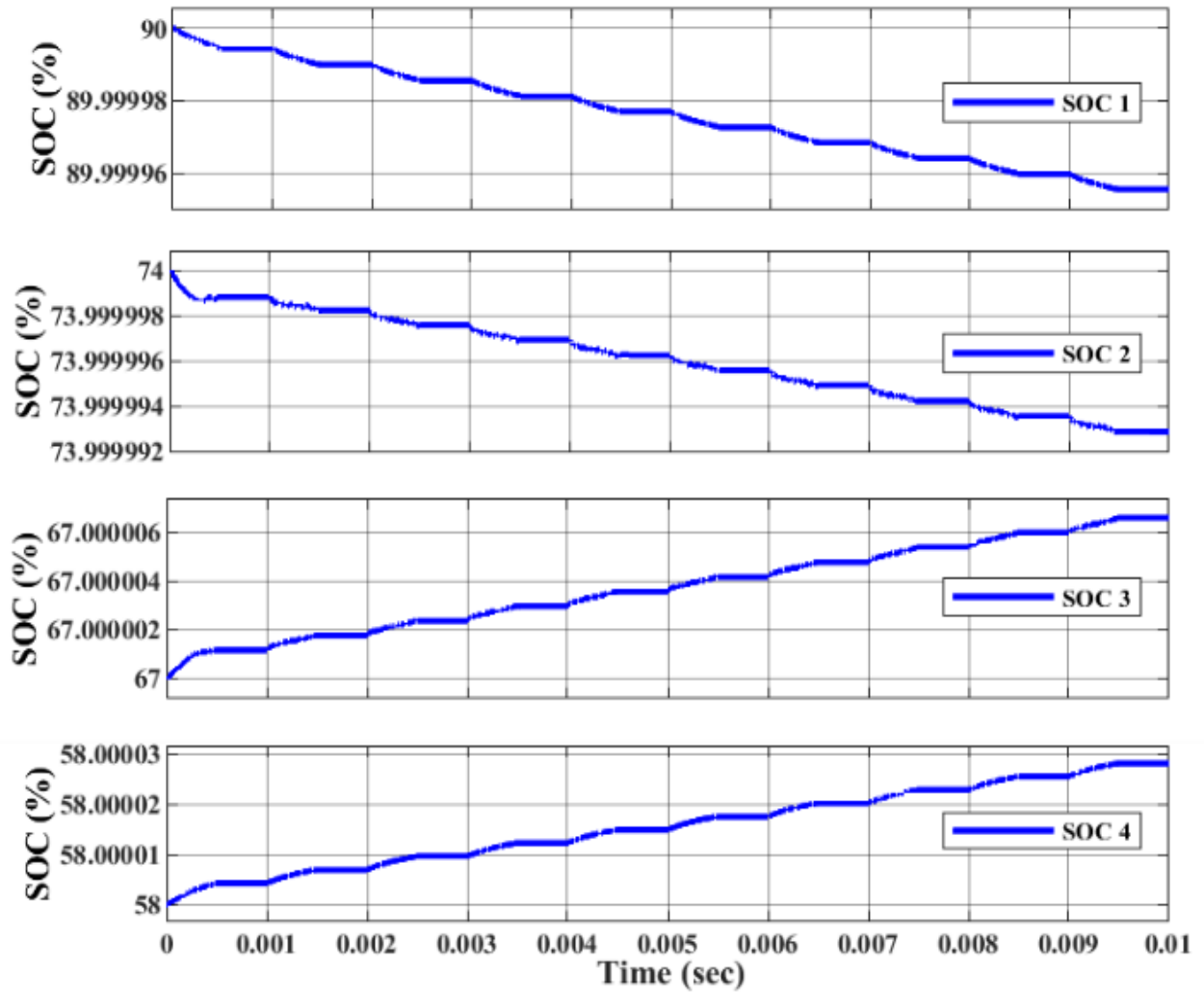


Fig. 6.12 SOC waveform for case I with delay

6.3.2 Case II

In case 2, SOC levels are randomly positioned, with the highest and the lowest SOC level of the battery are jumbled up and are not at extreme ends of the string. The average SOC levels of each group, as well as their differences, are determined using the suggested technique, and respective leg switches are turned on. M_{L1} , M_{L2} , and M_{H3} are thus operated in the appropriate legs of MCBB, whereas M_{H1} , M_{H2} , and M_{L3} are kept switched off. According to [55], leg 1 low side MOSFET will operate and tend to diverge the SOC levels and voltage differential from the average value, resulting in failure to deliver. The MCBB equalizer is simulated using MATLAB for case II. The suggested MCBB follows targeted equalization and the SOC levels of the batteries converge to their average SOC value as per the proposed algorithm, as shown in Fig. 6.15 and Fig. 6.13

shows the real time voltages for this case. Because M_{L_1} , M_{L_2} , and M_{H_3} switches work for case II, as Fig. 6.14 illustrates the current in L_{T_1} and L_{T_2} are in negative direction, while current in L_{T_3} is in positive direction as per the current convention taken. The equalization is faster which is only feasible with the flexibility of operating all legs at the same time.

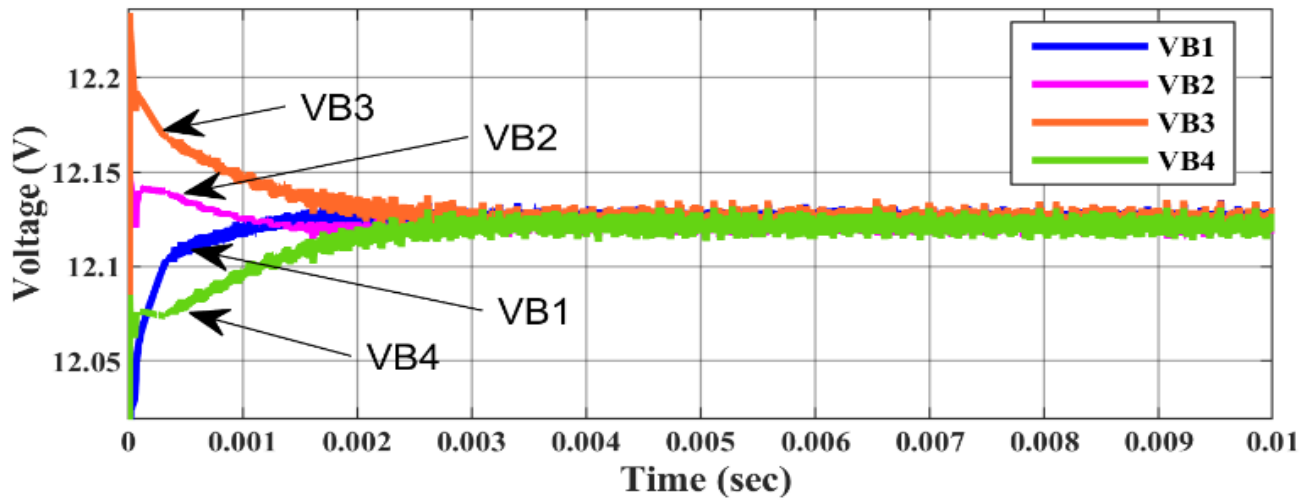


Fig. 6.13 Real time voltage waveform for case II

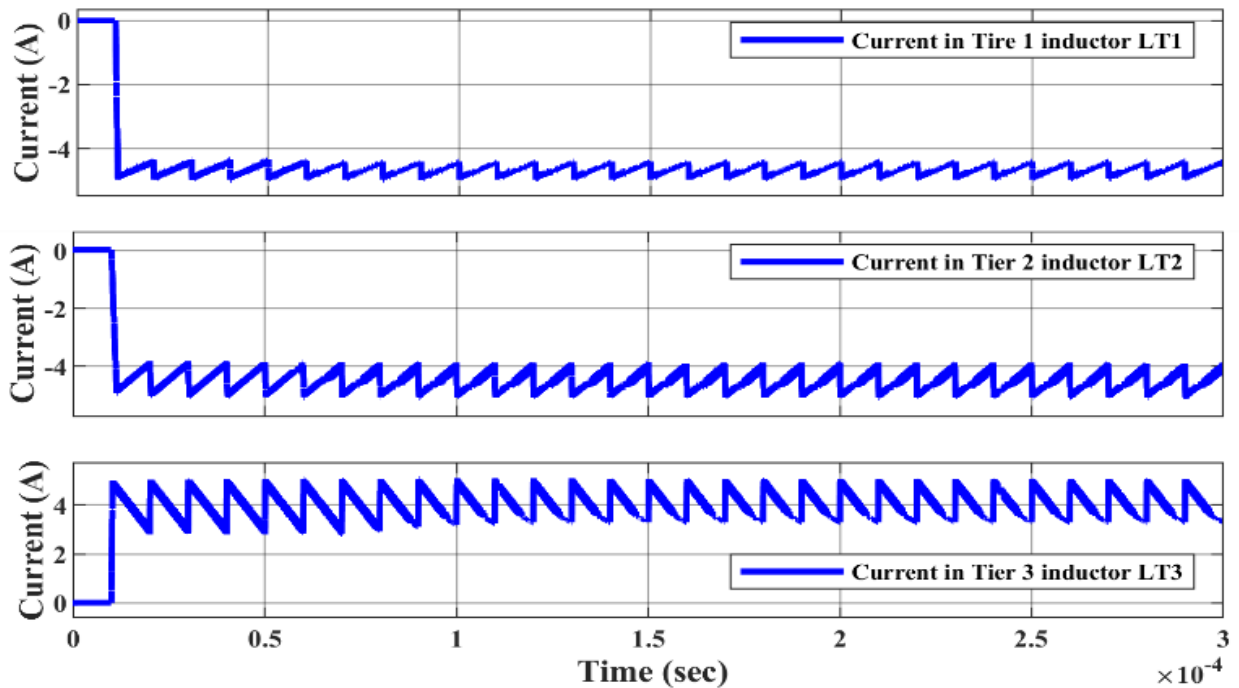


Fig. 6.14 Current waveform for case II

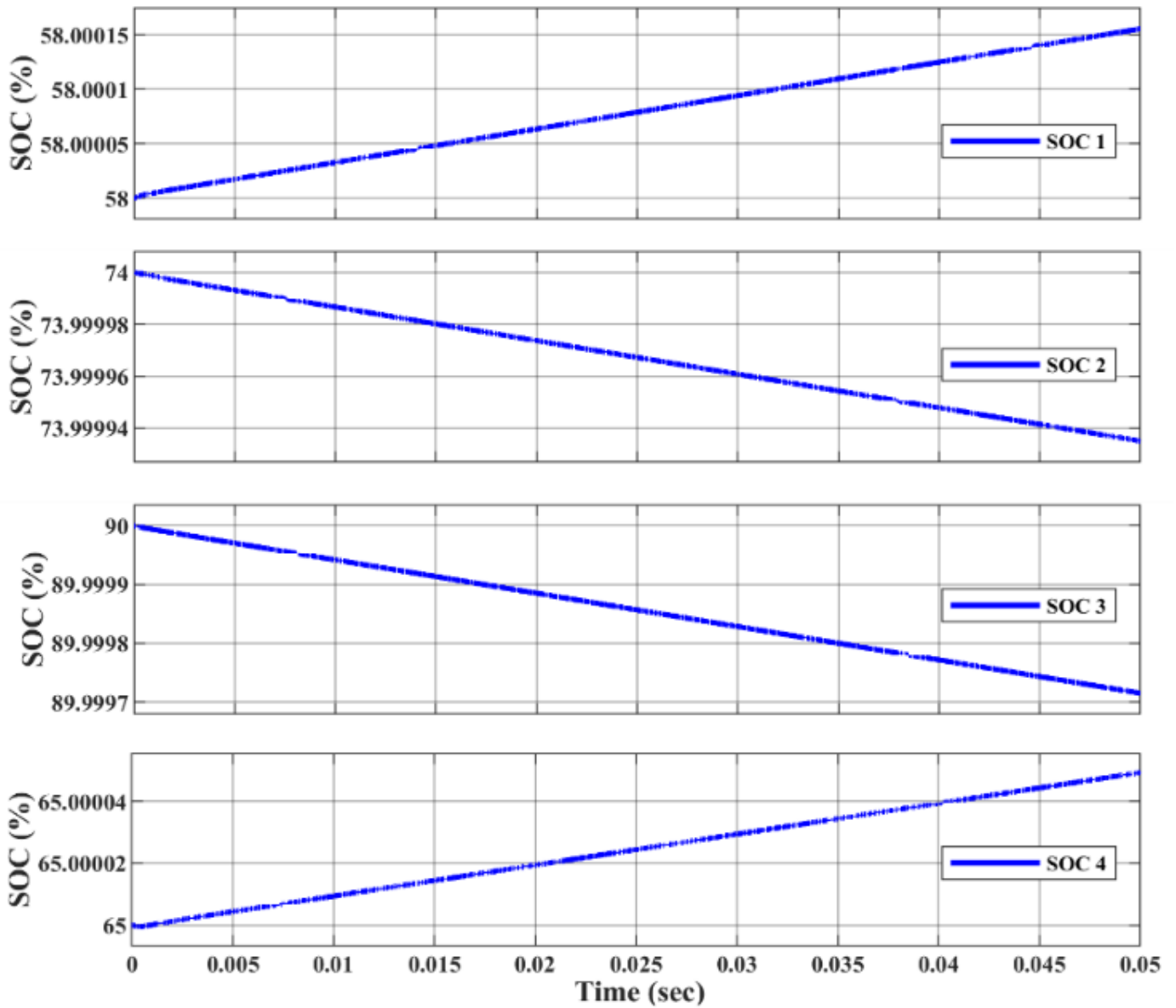


Fig. 6.15 SOC waveform for case II

The results show that MCBB can balance batteries with jumbled positioning of SOC levels with increased speed as well as targeted balancing with high efficiency using parallel routes with low and high side MOSFETs.

6.4 Comparison of Proposed Equalizer with Other Equalizer Based on Number of Components Used

The comparative analysis for the proposed equalizers is done with other similar buck-boost converter voltage equalizers for four batteries in a string. The comparison is done between equalizers of [51] Yanqin Zhang, [52] Shungang Xu, [53] Nguyen-Nghia Do, [54] XinBo Liu, [55] Shun-Chung Wang, proposed equalizer MMBE and MCBB. The parameters considered for comparison are listed below:

- If the equalizer supports targeted battery equalization and energy transfer from any cell to any cell in the string.
- The number of low side MOSFETs used in the equalizer for four cells in the string.
- The number of high side MOSFETs used in the equalizer for four cells in the string.
- Number of inductors used in the equalizer for four cells in the string.
- Number of diodes used in the equalizer for four cells in the string
- Number of high side and low side gate drivers used. Our proposed equalizers uses a single low side ground referred three channel gate drivers for all the three low side MOSFETs. It reduces the overall cost and also reduces the number of auxiliary supplies needed.
- Number of auxiliary supplies needed for four cells in the string
- Whether the equalizer is current controlled or not. Equalizers from [51], [52], [53], [55] derives the duty cycle from a predefined current value. This duty cycle value does not maintain the balancing balancing current at the designed value and thus there is not feedback for controlling
- current. Some of them also poses high current ripples and this produces more noise and losses.
- If voltage sensor is required or not for operating the equalizer.

TABLE 6.6 COMPARITIVE STUDY OF MMBE AND MCBB WITH OTHER EQUALIZERS

Equalizer / Reference Number	Targed Battery Balancing	Low Side Mosfets	High Side Mosfets	Inductors	Diodes	Gate Drivers	Auxiliary Supplies	Current Controlled	Voltage Sensors Required
[51] Yanqin Zhang	Partial	2	4	3	0	4- Isolated High Side 2- Ground Referred	6	No	Yes
[52] Shungang Xu	Partial	1	3	4	4	3- Isolated High Side 1- Ground Referred	4	No	Yes
[53] Nguyen-Nghia Do	No	2	4	2	0	4- Isolated High Side 2- Ground Referred	6	No	Yes
[54] XinBo Liu	No	1	3	3	0	3- Isolated High Side 1- Ground Referred	4	Yes	Yes
[55] Shun-Chung Wang	No	3	3	3	0	3- Isolated High Side 3- Ground Referred	6	No	Yes
MMBE	Yes	3	3	3 – mutually coupled	3	3- Isolated High Side 1- Ground Referred 3 channel non isolated	4	Yes	No (Ground referred differential 1 quad-opam)
MCBB	Yes	3	3	3 - mutually coupled	6	3- Isolated High Side 1- Ground Referred 3 channel non isolated	4	Yes	No (Ground referred differential 1 quad-opam)

CHAPTER 7

CONCLUSION AND FUTURE SCOPE OF WORK

7.1 Conclusion

With ambitious goals to increase renewable penetration in the main system, energy storage has emerged as a critical alternative for integrating it into the grid today. Large capacity batteries connected in series are increasingly being employed in large-scale energy storage power plants. The batteries are highly costly, and the battery life is short.

As a result, one significant aim is to increase battery consumption and life time. Unfortunately, in real applications, battery imbalances typically arise in series packs due to various intrinsic properties, resulting in a reduction in series battery pack capacity and reduced battery usage. Many equalisation circuits and control methods are reported to balance the battery voltages and boost life time, but almost all of them uses a high number of high side mosfets and thus corresponding high side isolated gate drivers and auxiliary supply. Many of them transfer energy in only one direction and doesnot support bidirectional and targeted battery balancing.

This study was undertaken with the motive of making the equalization circuit more efficient and making the control method flexible, clear and versatile. Two novel, multilevel multilooped equalization topologies for bidirectional targeted battery balancing based on buck-boost converter and its corresponding switching algorithm and dual loop control strategy is proposed in this thesis. The equalizers were tested for four lead acid batteries in series and validated for two different test cases for different SOC levels of the batteries positioned randomly in the string. A complete in-depth analysis was undertaken to evaluate all the possible test cases based on different SOC levels and its corresponding batteries position in the string. The results derived were very

encouraging with improved targeted cell balancing with control over balancing current. The most attractive feature of the research work is its ability to run without voltage sensor and the voltage can be sensed using ground referred differential op-amps. The methodology proposed is highly flexible, modular and cost-effective, capable of being applied to any battery energy storage system irrespective of the type of battery used.

The main highlights of the proposed equalizers MMBE and MCBB are listed below:

- Bidirectional energy flow within the string is achieved due to the converter topology.
- Targeted battery balancing is achieved as all the PELs are operated simultaneously and independently. Moreover the auxiliary circuits aid the targeted battery balancing. It is also effective with jumbled positioning of SOC levels if the cells in the string.
- Faster balancing is possible because all the PELs operate simultaneously.
- Speed of balancing can be modified as the balancing current can be controlled in the design. More the value of balancing current, quicker the balancing.
- No circulating current is allowed within the PELs due to the placement of mutual inductance that interlinks PELs.
- It is cost-effective and hardware compliant as it uses fewer number of high side MOSFETs, isolated gate drivers and auxiliary supplies.
- No voltage sensors required for this topology and a single ground referred differential quad op-amp can be used for four batteries in a string.

7.2 FUTURE SCOPE OF WORK

The future research potential for battery energy storage is both exciting and promising. Battery voltage equalizers play a crucial role in determining the performance and lifetime of battery pack. Different types of voltage equalisers have been investigated, and some new topologies have been built based on existing topologies that have been modified in order to build superior topologies. Based on the results of the completed research and report, a viable field for additional exploration is offered below.

-
- Hardware implementation of the equalizers can be done and its results can be compared with the presented simulation results to check the effectiveness of both the proposed equalizers MMBE and MCBB.
 - Soft switching method can be implemented in both the proposed topologies which would further improve the efficiency of the equalizers.
 - The proposed equalizers can be used for other applications like hybrid energy storage systems (batteries and supercapacitor hybrid storage systems), electric vehicles, etc. as it is equally effective for other types of batteries.
 - Equalization during charging and discharging conditions can also be analysed for both the proposed converters.
 - Other optimization techniques can also be applied that take away the hassle of voltage controller and current controller PI tuning and make the switching and controlling system more simple, compact and easy to use.

REFERENCES

- [1] IEA (2019), World Energy Outlook 2019, IEA, Paris <https://www.iea.org/reports/world-energy-outlook-2019>
- [2] S.H. Saeed and D.K.Sharma "Non-Conventional Energy Resources" S.kataria and Sons,,New Delhi, Second edition:2008-209;pp-3-4.
- [3] W. A. Kamal "Improving energy efficiency — The cost-effective way to mitigate global warming", Energy conversion and Management, vol. 38, pp. 39-59, 1997
- [4] IEA (2022), Renewable Energy Market Update - May 2022, IEA, Paris <https://www.iea.org/reports/renewable-energy-market-update-may-2022>
- [5] IEA (2021), India Energy Outlook 2021, IEA, Paris <https://www.iea.org/reports/india-energy-outlook-2021>
- [6] IEA (2020), India 2020, IEA, Paris <https://www.iea.org/reports/india-2020>
- [7] Power System Operation Corporation Ltd. (2016). Role of SRLDC. Retrieved from: <http://www.srldc.org/Role%20Of%20SRLDC.aspx>
- [8] J. Qi and D. Dah-Chuan Lu, "Review of battery cell balancing techniques," 2014 Australasian Universities Power Engineering Conference (AUPEC), 2014, pp. 1-6, doi: 10.1109/AUPEC.2014.6966514.
- [9] Daowd Mohamed, Omar Noshin, Van Den Bossche Peter, Van Mierlo Joeri. A review of passive and active battery balancing based on MATLAB/Simulink. Int Rev Electr Eng 2011;6(7):2974–89.
- [10] Rui LING, Lizhi WANG, Xueli HUANG, Qiang DAN, Jie ZHANG. A Review of Equalization Topologies for Lithium-ion Battery Packs. In: Proceedings of the 34th Chinese Control Conference. Hangzhou, China; p. 7922–27; 7/2015.
- [11] Park HS, Kim CH, Park KB, Moon GW, Lee JH. Design of a charge equalizer based on battery modularization. IEEE Trans Veh Technol 2009;58(7):3216–23.
- [12] Kim Moon-Young, Kim Jun-Ho, Moon Gun-Woo. Center-cell concentration structure of a cell-to-cell balancing circuit with a reduced number of switches. IEEE Trans Power Electron 2014;29(10):5285–97.

- [13] Gallardo-Lozano Javier, Romero-Cadaval Enrique, Milanes-Montero M Isabel, Guerrero-Martinez Miguel A. Battery equalization active methods: review article. *J Power Sources* 2014;246:934–49.
- [14] Baronti Federico, Roncella Roberto, Saletti Roberto. Performance comparison of active balancing techniques for lithium-ion batteries. *J Power Sources* 2014;267:603–9.
- [15] Gallardo-Lozano J, Romero-Cadaval E, Milanes-Montero MI, Guerrero-Martinez MA. Battery equalization active methods. *J Power Sources* 2014;246:934–49.
- [16] Moore S, Schneider P. A Review of Cell Equalization Methods for Lithium Ion and Lithium Polymer Battery Systems. in *Proceedings of the SAE 2001 World Congress*; 2001.
- [17] Thomas Stuart A, Zhu Wei. Fast equalization for large lithium ion batteries. *IEEE Aerosp Electron Syst Mag* 2009;24:27–31.
- [18] A. A. Ghotekar and B. E. Kushare, "Review Paper on Recent Active Voltage Balancing Methods for Supercapacitor Energy Storage System," 2019 5th International Conference On Computing, Communication, Control And Automation (ICCUBEA), 2019, pp. 1-5, doi: 10.1109/ICCUBEA47591.2019.9128470.
- [19] M. Daowd, N. Omar, P. Van Den Bossche and J. Van Mierlo, "Passive and active battery balancing comparison based on MATLAB simulation," 2011 IEEE Vehicle Power and Propulsion Conference, 2011, pp. 1-7, doi: 10.1109/VPPC.2011.6043010.
- [20] Gallardo-Lozano Javier, Romero-Cadaval Enrique, Milanes-Montero M Isabel, Guerrero-Martinez Miguel A. A novel active battery equalization control with online unhealthy cell detection and cell change decision. *J Power Sources* 2015;299:356–70.
- [21] Hua Yin, Cordoba-Arenas Andrea, Warner Nicholas, Rizzoni Giorgio. A multitime-scale state-of-charge and state-of-health estimation framework using non-linear predictive filter for lithium-ion battery pack with passive balance control. *J Power Sources* 2015;280:293–312.
- [22] Zhang Xiujuan, Liu Peide, Wang Darui. The design and implementation of smart battery management system balance technology. *J Converg Inf Technol* 2011;6(5):108–16.
- [23] Goodarzi S, Beiranvand R, Mousavi SM, Mohamadian M. A new algorithm for increasing balancing speed of switched-capacitor lithium-ion battery cell equalizers. *Power Electronics*,

Drives Systems & Technologies Conference (PEDSTC), 2015 6th, IEEE Conference Publications, p. 292–97; 2015.

- [24] Baughman AC, Ferdowsi M. Double-tiered switched-capacitor battery charge equalization technique. *IEEE Trans Ind Electron* 2008;55:2277–85.
- [25] Baughman A, Ferdowsi M. Double-tiered capacitive shuttling method for balancing series-connected batteries. *IEEE Conf Veh Power Propuls* 2005:109–13.
- [26] Daowd Mohamed, Omar Noshin, Van Den Bossche Peter, Van Mierlo Joeri. A review of passive and active battery balancing based on MATLAB/Simulink. *Int Rev Electr Eng* 2011;6(7):2974–89.
- [27] Hong-Sun P, Cho I-Ho K, Ki-Bum P, Gun-Woo M, Joong-Hui L. Design of a charge equalization based on battery modularization. *IEEE Trans Veh Technol* 2009;58:3938–46.
- [28] Kim Moon-Young, Kim Chol-Ho, Kim Jun-Ho, Moon Gun-Woo. A chain structure of switched capacitor for improved cell balancing speed of lithium-ion batteries. *IEEE Trans Ind Electron* 2014;61(8):3989–99.
- [29] Andrea D. Battery management systems for large lithium ion battery packs, 1st ed.. London, UK: Artech House; 2010. p. 22–110.
- [30] Sang-Hyun P, Tae-Sung K, Jin-Sik P, Gun-Woo M, Myung-Joong Y. A New Battery Equalizer Based on Buck-boost Topology. *IEEE 7th International Conf. on Power Electronics*, p. 962–65; 2007.
- [31] Imtiaz AbusalehM, Khan FaisalH, Kamath Hareesh. A Low-Cost Time Shared Cell Balancing Technique for Future Lithium-Ion Battery Storage System Featuring Regenerative Energy Distribution. *IEEE 26th Annual Applied Power Electronics Conference and Exposition (APEC)*, p. 792–99; 2011.
- [32] Park Sang-Hyun, Park Ki-Bum, Kim Hyoung-Suk, Moon Gun-Woo, Youn MyungJoong. Single-magnetic cell-to-cell charge equalization converter with reduced number of transformer windings. *Power Electron IEEE Trans* 2012;27(6):2900–11.
- [33] Phung TH, Crebier JC, Chureau A, Collet A, Van Nguyen NT. Optimized Structure for Next-to-Next Balancing of Series-Connected Lithium-ion Cells. *26th Annual IEEE Applied Power Electronics Conference and Exposition (APEC)*, p. 1374–81; 2011.

- [34] Daowd Mohamed, Omar Noshin, Van Den Bossche Peter, Van Mierlo Joeri. A review of passive and active battery balancing based on MATLAB/Simulink. *Int Rev Electr Eng* 2011;6(7):2974–89.
- [35] Einhorn M, Roessler W, Fleig J. Improved performance of serially connected Li-ion batteries with active cell balancing in electric vehicles. *IEEE Trans Veh Technol* 2011;60(6):2448–57.
- [36] Parky Kyung-Hwa, Kim Chol-Ho, Cho Hee-Keun, Seo Joung-Ki. Design considerations of a lithium ion Battery Management System (BMS) for the STSAT-3 satellite. *J Power Electron* 2010;10(2):210–7.
- [37] Li S, Mi C, Zhang M. A high-efficiency active battery-balancing circuit using multiwinding transformer. *Ind Appl IEEE Trans* 2013;49(2):198–207.
- [38] Hong-Sun P, Cho I-Ho K, Ki-Bum P, Gun-Woo M, Joong-Hui L. Design of a charge equalization based on battery modularization. *IEEE Trans Veh Technol* 2009;58:3938–46.
- [39] Sang-Hyun P, Tae-Sung K, Jin-Sik P, Gun-Woo M, Myung-Joong Y. A New Battery Equalizer Based on Buck-boost Topology. *IEEE 7th International Conf. on Power Electronics*, p. 962–65; 2007.
- [40] Moo CS, Hsieh YC, Tsai IS. Charge equalization series-connected batteries. *AerospElectron Syst IEEE Trans* 2013;39(2):704–10.
- [41] Lu Xi, Qian Wei, Peng Fang-Zheng. Modularized buck-boost + Cuk converter for high voltage series connected battery cells. *Applied Power Electronics Conference and Exposition (APEC), 2012 Twenty-Seventh Annual IEEE*; p. 2272,2278; 2/2012.
- [42] Wu Tsung-Hsi, Chang Chu-Shen, Moo Chin-Sien. A charging scenario for parallel buck-boost battery power modules with full power utilization and charge equalization. *Industrial Technology (ICIT), 2015 IEEE International Conference on*, p. 860–65; 2015.
- [43] Uno Masatoshi, Kukita Akio. Single-switch constant-power equalization charger based on multi-stacked buck-boost converters for series-connected supercapacitors in satellite power system. *2011 IEEE power electronics and drive systems conference*, p. 1158–65; 2011.
- [44] Chen Woei-Luen, Cheng Shin-Rung. Optimal charge equalisation control for series connected batteries. *Gener Transm Distrib IET* 2013;7(8):843–54.

- [45] Venmathi M, Ramaprabha R. A comprehensive survey on multi-port bidirectional dc-dc converters for renewable energy systems. *ARNP J Eng Appl Sci* 2013;8(5):348–56.
- [46] Simon M, Murken M, Augustin C, Pforr J. Multi-Port Converter with bidirectional energy flow for automotive energy net applications. *Power Electron Appl* 2014:1–10.
- [47] Gotwald T, Ye Z, Stuart . Equalization of EV and HEV batteries with a ramp converter. *IEEE Trans Aerosp Electron Syst* 1997;33(1):307–12.
- [48] Kim JW, Shin JW, Ik Ha J. Cell balancing control using adjusted filters in flyback converter with single switch. 2013 IEEE Energy Conversion Congress and Exposition (ECCE); p. 287–91; 9/2013.
- [49] Imtiaz AM, Khan FH. Time shared flyback converter based regenerative cell balancing technique for series connected Li-ion battery strings. *IEEE Trans Power Electron* 2013;28(12):5960–75.
- [50] Kim Jin-Woong, Ha Jung-Ik. Cell balancing control of single switch flyback converter using generalized filters. *Applied Power Electronics Conference and Exposition (APEC)*, p. 3273–77; 2014.
- [51] Y. Zhang and R. Yang, "An Improved Buck-Boost Circuit Equalization Method for Series Connected Battery Packs," 2021 IEEE 4th International Electrical and Energy Conference (CIEEC), 2021, pp. 1-6, doi: 10.1109/CIEEC50170.2021.9510474.
- [52] S. Xu, K. Gao, G. Zhou, X. Zhang and S. Mao, "A Novel Battery Equalizer Based on Buck-Boost Converters for Series-connected batteries," 2020 IEEE 9th International Power Electronics and Motion Control Conference (IPEMC2020-ECCE Asia), 2020, pp. 219-223, doi: 10.1109/IPEMC-ECCEAsia48364.2020.9367650.
- [53] N. -N. Do, H. -J. Chiu and Y. -C. Hsieh, "A Novel Symmetric Battery Equalizer Topology Based on Bidirectional DC/DC Converter for Series-Connected Lithium-ion Cells," 2020 3rd International Conference on Power and Energy Applications (ICPEA), 2020, pp. 6-9, doi: 10.1109/ICPEA49807.2020.9280139.
- [54] X. Liu, Z. Gao, X. Huang and Y. Zou, "Large Equalization Current Control Strategy for Series Connected Battery Packs Based on Buck-Boost Converter," 2018 International Power Electronics Conference (IPEC-Niigata 2018 -ECCE Asia), 2018, pp. 3455-3459, doi: 10.23919/IPEC.2018.8507560.

- [55] S. -C. Wang, G. -J. Chen, H. -Y. Pai and Y. -H. Liu, "A Fast Equalizer with Mechanisms of Bidirectional Energy Transfer and Balancing Current Control," 2020 3rd IEEE International Conference on Knowledge Innovation and Invention (ICKII), 2020, pp. 313-316, doi: 10.1109/ICKII50300.2020.93189
- [56] Y. Shang, B. Xia, C. Zhang, N. Cui, J. Yang and C. Mi, "An automatic battery equalizer based on forward and flyback conversion for series-connected battery strings," 2017 IEEE Applied Power Electronics Conference and Exposition (APEC), 2017, pp. 3218-3222, doi: 10.1109/APEC.2017.7931157.
- [57] J. Shin, G. Seo, C. Chun and B. Cho, "Selective flyback balancing circuit with improved balancing speed for series connected Lithium-ion batteries," The 2010 International Power Electronics Conference - ECCE ASIA -, 2010, pp. 1180-1184, doi: 10.1109/IPEC.2010.5543502.
- [58] K. Yu, Y. Shang, X. Wang, N. Wang, B. Duan and C. Zhang, "A Multi-Cell-to-Multi-Cell Equalizer for Series-Connected Batteries Based on Flyback Conversion," 2019 3rd Conference on Vehicle Control and Intelligence (CVCI), 2019, pp. 1-5, doi: 10.1109/CVCI47823.2019.8951748.
- [59] Y. Shang, B. Xia, C. Zhang, N. Cui, J. Yang and C. Mi, "An automatic battery equalizer based on forward and flyback conversion for series-connected battery strings," 2017 IEEE Applied Power Electronics Conference and Exposition (APEC), 2017, pp. 3218-3222, doi: 10.1109/APEC.2017.7931157.
- [60] Y. Shang, N. Cui, B. Duan and C. Zhang, "A Global Modular Equalizer Based on Forward Conversion for Series-Connected Battery Strings," in IEEE Journal of Emerging and Selected Topics in Power Electronics, vol. 6, no. 3, pp. 1456-1469, Sept. 2018, doi: 10.1109/JESTPE.2017.2768388.

PUBLICATIONS

- [1] Multimode-Multilevel Bidirectional Converter for Target Battery Equalization in a Tandem Connected Battery Units –
ACCEPTED - The 2022 IEEE 13th International symposium Power Electronics for Distributed Generation Systems (PEDG), scheduled in Kiel, Germany from 26-29 June, 2022.
- [2] Multi-Looped Current Controlled Bidirectional Bridge Converter for Targeted Battery Equalization
ACCEPTED - EPE'22 ECCE EUROPE 24th European Conference on Power Electronics and Applications scheduled in Hannover, Germany, from 5 to 9 September 2022.